EUROPEAN ORGANISATION FOR NUCLEAR RESEARCH

CERN-PPE/95-090
23 June 1995

Measurement of the Average b-Baryon Lifetime and the Product Branching Ratio $f(\mathrm{b} \to \Lambda_\mathrm{b}) \cdot BR(\Lambda_\mathrm{b} \to \Lambda \ell^- \bar{\nu} \mathrm{X})$

OPAL Collaboration

Abstract

The average lifetime of b-flavoured baryons measured with the OPAL detector is updated to include data collected between 1990 and 1994 at LEP. Bottom-flavoured baryons that decay semileptonically and produce a Λ baryon are identified through the correlation of the baryon number of the Λ and the electric charge of the lepton. To measure the lifetime, the decay point of the b baryon is estimated by the Λ-lepton vertex, and the observed distribution of decay lengths is fitted simultaneously in 874 right-sign and 384 wrong-sign combinations. In a separate method, the impact parameter distribution of the leptons is fitted in a subset of these data. When the two results are combined, taking correlations into account, the average b-baryon lifetime is found to be

$$\tau = 1.16 \pm 0.11\,(\mathrm{stat.}) \pm 0.06\,(\mathrm{syst.})\ \mathrm{ps}.$$

Using the same data, the product branching ratio is measured to be

$$f(\mathrm{b} \to \Lambda_\mathrm{b}) \cdot BR(\Lambda_\mathrm{b} \to \Lambda \ell^- \bar{\nu} \mathrm{X}) = (2.91 \pm 0.23\,(\mathrm{stat.}) \pm 0.25\,(\mathrm{syst.})) \cdot 10^{-3},$$

where the symbol $f(\mathrm{b} \to \Lambda_\mathrm{b})$ is the fraction of b quarks from Z^0 decays forming b baryons, Λ_b represents all b-flavoured baryons and ℓ is either an electron or a muon.

(Submitted to Zeitschrift für Physik C)

The OPAL Collaboration

R. Akers[16], G. Alexander[23], J. Allison[16], N. Altekamp[5], K. Ametewee[25], K.J. Anderson[9], S. Anderson[12], S. Arcelli[2], S. Asai[24], D. Axen[29], G. Azuelos[18,a], A.H. Ball[17], E. Barberio[26], R.J. Barlow[16], R. Bartoldus[3], J.R. Batley[5], G. Beaudoin[18], J. Bechtluft[14], A. Beck[23], G.A. Beck[13], C. Beeston[16], T. Behnke[27], K.W. Bell[20], G. Bella[23], S. Bentvelsen[8], P. Berlich[10], S. Bethke[14], O. Biebel[14], I.J. Bloodworth[1], P. Bock[11], H.M. Bosch[11], M. Boutemeur[18], S. Braibant[12], P. Bright-Thomas[25], R.M. Brown[20], A. Buijs[8], H.J. Burckhart[8], C. Burgard[27], R. Bürgin[10], P. Capiluppi[2], R.K. Carnegie[6], A.A. Carter[13], J.R. Carter[5], C.Y. Chang[17], C. Charlesworth[6], D.G. Charlton[1,b], S.L. Chu[4], P.E.L. Clarke[15], J.C. Clayton[1], S.G. Clowes[16], I. Cohen[23], J.E. Conboy[15], O.C. Cooke[16], M. Cuffiani[2], S. Dado[22], C. Dallapiccola[17], G.M. Dallavalle[2], C. Darling[31], S. De Jong[12], L.A. del Pozo[8], H. Deng[17], M.S. Dixit[7], E. do Couto e Silva[12], J.E. Duboscq[8], E. Duchovni[26], G. Duckeck[8], I.P. Duerdoth[16], U.C. Dunwoody[8], J.E.G. Edwards[16], P.G. Estabrooks[6], H.G. Evans[9], F. Fabbri[2], B. Fabbro[21], M. Fanti[2], P. Fath[11], F. Fiedler[12], M. Fierro[2], M. Fincke-Keeler[28], H.M. Fischer[3], R. Folman[26], D.G. Fong[17], M. Foucher[17], H. Fukui[24], A. Fürtjes[8], P. Gagnon[6], A. Gaidot[21], J.W. Gary[4], J. Gascon[18], S.M. Gascon-Shotkin[17], N.I. Geddes[20], C. Geich-Gimbel[3], S.W. Gensler[9], F.X. Gentit[21], T. Geralis[20], G. Giacomelli[2], P. Giacomelli[4], R. Giacomelli[2], V. Gibson[5], W.R. Gibson[13], J.D. Gillies[20], D.M. Gingrich[30,a], J. Goldberg[22], M.J. Goodrick[5], W. Gorn[4], C. Grandi[2], E. Gross[26], G.G. Hanson[12], M. Hansroul[8], M. Hapke[13], C.K. Hargrove[7], P.A. Hart[9], C. Hartmann[3], M. Hauschild[8], C.M. Hawkes[8], R. Hawkings[8], R.J. Hemingway[6], G. Herten[10], R.D. Heuer[8], J.C. Hill[5], S.J. Hillier[8], T. Hilse[10], P.R. Hobson[25], D. Hochman[26], R.J. Homer[1], A.K. Honma[28,a], R. Howard[29], R.E. Hughes-Jones[16], D.E. Hutchcroft[5], P. Igo-Kemenes[11], D.C. Imrie[25], A. Jawahery[17], P.W. Jeffreys[20], H. Jeremie[18], M. Jimack[1], A. Joly[18], M. Jones[6], R.W.L. Jones[8], P. Jovanovic[1], J. Kanzaki[24], D. Karlen[6], K. Kawagoe[24], T. Kawamoto[24], R.K. Keeler[28], R.G. Kellogg[17], B.W. Kennedy[20], B.J. King[8], J. King[13], J. Kirk[29], S. Kluth[5], T. Kobayashi[24], M. Kobel[10], D.S. Koetke[6], T.P. Kokott[3], S. Komamiya[24], R. Kowalewski[8], T. Kress[11], P. Krieger[6], J. von Krogh[11], P. Kyberd[13], G.D. Lafferty[16], H. Lafoux[8], R. Lahmann[17], W.P. Lai[19], D. Lanske[14], J. Lauber[8], J.G. Layter[4], A.M. Lee[31], E. Lefebvre[18], D. Lellouch[26], J. Letts[2], L. Levinson[26], S.L. Lloyd[13], F.K. Loebinger[16], G.D. Long[17], B. Lorazo[18], M.J. Losty[7], J. Ludwig[10], A. Luig[10], A. Malik[21], M. Mannelli[8], S. Marcellini[2], C. Markus[3], A.J. Martin[13], J.P. Martin[18], T. Mashimo[24], W. Matthews[25], P. Mättig[3], J. McKenna[29], E.A. Mckigney[15], T.J. McMahon[1], A.I. McNab[13], F. Meijers[8], S. Menke[3], F.S. Merritt[9], H. Mes[7], A. Michelini[8], G. Mikenberg[26], D.J. Miller[15], R. Mir[26], W. Mohr[10], A. Montanari[2], T. Mori[24], M. Morii[24], U. Müller[3], B. Nellen[3], B. Nijjhar[16], S.W. O'Neale[1], F.G. Oakham[7], F. Odorici[2], H.O. Ogren[12], N.J. Oldershaw[16], C.J. Oram[28,a], M.J. Oreglia[9], S. Orito[24], F. Palmonari[2], J.P. Pansart[21], G.N. Patrick[20], M.J. Pearce[1], P.D. Phillips[16], J.E. Pilcher[9], J. Pinfold[30], D.E. Plane[8], P. Poffenberger[28], B. Poli[2], A. Posthaus[3], T.W. Pritchard[13], H. Przysiezniak[30], M.W. Redmond[8], D.L. Rees[1], D. Rigby[1], M.G. Rison[5], S.A. Robins[13], N. Rodning[30], J.M. Roney[28], E. Ros[8], A.M. Rossi[2], M. Rosvick[28], P. Routenburg[30], Y. Rozen[8], K. Runge[10], O. Runolfsson[8], D.R. Rust[12], M. Sasaki[24], C. Sbarra[2], A.D. Schaile[8], O. Schaile[10], F. Scharf[3], P. Scharff-Hansen[8], P. Schenk[4], B. Schmitt[3], M. Schröder[8], H.C. Schultz-Coulon[10], M. Schulz[8], P. Schütz[3], J. Schwiening[3], W.G. Scott[20], M. Settles[12], T.G. Shears[16], B.C. Shen[4], C.H. Shepherd-Themistocleous[7], P. Sherwood[15], G.P. Siroli[2], A. Skillman[15], A. Skuja[17], A.M. Smith[8], T.J. Smith[28], G.A. Snow[17], R. Sobie[28], S. Söldner-Rembold[10], R.W. Springer[30], M. Sproston[20], A. Stahl[3], M. Starks[12], C. Stegmann[10], K. Stephens[16], J. Steuerer[28], B. Stockhausen[3], D. Strom[19], P. Szymanski[20], R. Tafirout[18], P. Taras[18], S. Tarem[26], M. Tecchio[9], P. Teixeira-Dias[11], N. Tesch[3], M.A. Thomson[8], E. von Törne[3], S. Towers[6], M. Tscheulin[10], T. Tsukamoto[24], A.S. Turcot[9], M.F. Turner-Watson[8], P. Utzat[11], R. Van Kooten[12], G. Vasseur[21], P. Vikas[18], M. Vincter[28], F. Wäckerle[10], A. Wagner[27], D.L. Wagner[9], C.P. Ward[5], D.R. Ward[5], J.J. Ward[15], P.M. Watkins[1], A.T. Watson[1], N.K. Watson[7], P. Weber[6], P.S. Wells[8], N. Wermes[3], B. Wilkens[10], G.W. Wilson[27], J.A. Wilson[1], T. Wlodek[26], G. Wolf[26], S. Wotton[11], T.R. Wyatt[16], G. Yekutieli[26], V. Zacek[18], W. Zeuner[8], G.T. Zorn[17].

[1]School of Physics and Space Research, University of Birmingham, Birmingham B15 2TT, UK

[2]Dipartimento di Fisica dell' Università di Bologna and INFN, I-40126 Bologna, Italy

[3]Physikalisches Institut, Universität Bonn, D-53115 Bonn, Germany

[4]Department of Physics, University of California, Riverside CA 92521, USA

[5]Cavendish Laboratory, Cambridge CB3 0HE, UK

[6]Carleton University, Department of Physics, Colonel By Drive, Ottawa, Ontario K1S 5B6, Canada

[7]Centre for Research in Particle Physics, Carleton University, Ottawa, Ontario K1S 5B6, Canada
[8]CERN, European Organisation for Particle Physics, CH-1211 Geneva 23, Switzerland
[9]Enrico Fermi Institute and Department of Physics, University of Chicago, Chicago IL 60637, USA
[10]Fakultät für Physik, Albert Ludwigs Universität, D-79104 Freiburg, Germany
[11]Physikalisches Institut, Universität Heidelberg, D-69120 Heidelberg, Germany
[12]Indiana University, Department of Physics, Swain Hall West 117, Bloomington IN 47405, USA
[13]Queen Mary and Westfield College, University of London, London E1 4NS, UK
[14]Technische Hochschule Aachen, III Physikalisches Institut, Sommerfeldstrasse 26-28, D-52056 Aachen, Germany
[15]University College London, London WC1E 6BT, UK
[16]Department of Physics, Schuster Laboratory, The University, Manchester M13 9PL, UK
[17]Department of Physics, University of Maryland, College Park, MD 20742, USA
[18]Laboratoire de Physique Nucléaire, Université de Montréal, Montréal, Quebec H3C 3J7, Canada
[19]University of Oregon, Department of Physics, Eugene OR 97403, USA
[20]Rutherford Appleton Laboratory, Chilton, Didcot, Oxfordshire OX11 0QX, UK
[21]CEA, DAPNIA/SPP, CE-Saclay, F-91191 Gif-sur-Yvette, France
[22]Department of Physics, Technion-Israel Institute of Technology, Haifa 32000, Israel
[23]Department of Physics and Astronomy, Tel Aviv University, Tel Aviv 69978, Israel
[24]International Centre for Elementary Particle Physics and Department of Physics, University of Tokyo, Tokyo 113, and Kobe University, Kobe 657, Japan
[25]Brunel University, Uxbridge, Middlesex UB8 3PH, UK
[26]Particle Physics Department, Weizmann Institute of Science, Rehovot 76100, Israel
[27]Universität Hamburg/DESY, II Institut für Experimental Physik, Notkestrasse 85, D-22607 Hamburg, Germany
[28]University of Victoria, Department of Physics, P O Box 3055, Victoria BC V8W 3P6, Canada
[29]University of British Columbia, Department of Physics, Vancouver BC V6T 1Z1, Canada
[30]University of Alberta, Department of Physics, Edmonton AB T6G 2J1, Canada
[31]Duke University, Department of Physics, Durham, NC 27708-0305, USA

[a]Also at TRIUMF, Vancouver, Canada V6T 2A3
[b] Royal Society University Research Fellow

1 Introduction

The b-quark lifetime and its semileptonic branching ratio are important for the determination of the CKM mixing parameter $V_{\rm cb}$. The estimation of heavy quark lifetimes from the observed weakly decaying b-hadron lifetimes is complicated by the influence in the decay process of the other quarks in the hadron, called spectator quarks. Because of the large mass of the b quark, the influence of the spectator quarks is thought to be small in b-hadron decays. As a result, lifetimes of the different weakly decaying b-flavoured hadrons are expected to be equal to within 10–20% [1]. The greatest variation is predicted for b baryons, which are expected to have shorter lifetimes than the B mesons since the non-spectator W-exchange diagram is helicity suppressed in mesons but not in baryons. It is important to verify this prediction in the context of calculations invoking heavy quark mass expansions in the framework of QCD. Non-spectator effects will also influence the semileptonic branching ratio of b baryons. This branching ratio is expected to be smaller for b baryons than for B mesons [2]. Unfortunately, the measurement of the semileptonic branching ratio at LEP is complicated by the unknown total b-baryon production rate in $\rm Z^0$ decays.

Experiments at the LEP and Tevatron colliders have provided precise measurements of the average b-hadron lifetime [3, 4], several exclusive b-hadron lifetimes [5, 6, 7, 8], and b baryon production rates [8]. This paper describes an improved measurement, using the OPAL detector, of the average b-baryon lifetime and the product branching ratio $f(\mathrm{b} \to \Lambda_\mathrm{b}) \cdot BR(\Lambda_\mathrm{b} \to \Lambda \ell^- \bar{\nu} \mathrm{X})$, where $f(\mathrm{b} \to \Lambda_\mathrm{b})$ is the fraction of b quarks forming b baryons from $\rm Z^0$ decays. Events that contain decay chains of the form[1],

$$\begin{array}{l} \Lambda_\mathrm{b}^0 \to \Lambda_\mathrm{c}^+ \, \ell^- \, \bar{\nu} \;\; X \\ \qquad \hookrightarrow \Lambda \; X \\ \qquad\quad \hookrightarrow \mathrm{p} \; \pi^- \end{array} \qquad \text{and} \qquad \begin{array}{l} \Xi_\mathrm{b}^0 \to \Xi_\mathrm{c}^+ \, \ell^- \, \bar{\nu} \;\; X \\ \qquad \hookrightarrow \Lambda \; X \\ \qquad\quad \hookrightarrow \mathrm{p} \; \pi^-. \end{array}$$

are studied. The correlation of a Λ with a negatively-charged lepton or a $\bar{\Lambda}$ with a positively-charged lepton can indicate the presence of a semileptonic b-baryon decay, as used by OPAL in Ref. [9]. The other charge combinations ($\bar{\Lambda}$-ℓ^- and Λ-ℓ^+) are used to characterize and estimate the level of background. Only the ground-state b baryons Λ_b^0 (quark content: bud), Ξ_b^0 (bsu), Ξ_b^- (bsd), and Ω_b^- (bss) are expected to decay weakly [1]. The production of Ξ_b and especially Ω_b^- are believed to be suppressed; therefore, the symbol Λ_b will be used in this paper to refer to all b baryons, while the symbol Λ_b^0 will be used to refer to the particular b baryon state with quark content (bud). This analysis actually measures the average lifetime and product branching ratio of weakly decaying b baryons weighted by their different production rates in $\rm Z^0$ decays, branching ratios, and detection efficiencies.

OPAL's previous value [10] of $1.05^{+0.23}_{-0.20} \pm 0.08$ ps for the average b-baryon lifetime was measured from data collected between 1990 and 1992 using the distribution of decay lengths between the primary event vertex and the vertex formed by the lepton and Λ. In addition to updating the decay length measurement to include 1993 and 1994 data, the analysis presented here also includes a lifetime measurement based on the impact parameters of the leptons from b-baryon semileptonic decay. This paper also updates the published OPAL product branching ratio measurement [9], which was obtained with the data recorded in the years 1990 and 1991. The inclusion of data collected up to the end of 1994 represents an approximate threefold increase in overall statistics for the lifetime measurement, and a ninefold increase for the product branching ratio. Other improvements include the use of high precision tracking information from the silicon microvertex detector, a more efficient set of electron identification criteria, and a slight modification of Λ selection criteria.

[1] Charge conjugate processes are implied throughout this paper.

In the following sections, the event selection is briefly described, as are the Monte Carlo samples used in the analysis. For the lifetime measurement, the decay length and impact parameter methods and the fitting procedures are described and checks with Monte Carlo simulations are presented. The results of the b-baryon lifetime measurements from the two methods are given, and estimates of systematic uncertainties are discussed. Finally, correlations between the methods, statistical and systematic, are considered, and the results of the two methods are combined for a single average b-baryon lifetime measurement where the average is over the different b baryon species. In the extraction of the product branching ratio, the determination of the selection efficiencies and their systematic uncertainties are first presented. Background sources are investigated and corrections to the background estimate described. The product branching ratio is determined, and the implications of this and the average b-baryon lifetime result are discussed.

2 The OPAL Detector

A detailed description of the OPAL detector can be found elsewhere [11]. The most important component for this analysis is the central tracking system composed of a precision vertex drift chamber and a large volume jet chamber. The jet chamber also provides ionization energy loss ($\mathrm{d}E/\mathrm{d}x$) measurements [12], and is surrounded by a set of chambers to measure the z-coordinate[2] of tracks as they exit the jet chamber. Since 1991, a high precision silicon microvertex detector [13] has been installed. It was operational for 73% of the data collected in 1991 and all of the data collected in 1992. For 1993, the silicon detector was upgraded [14] to supply in addition tracking information in the z-coordinate, but only r-ϕ silicon microvertex detector information is used for the analyses in this paper. This upgraded detector was operational for all of 1993 and 80% of the data collected in 1994. The impact parameter resolution in the x-y plane achieved for single tracks of momentum 45 GeV/c in $\mathrm{Z}^0 \to \mu^+\mu^-$ events is 18 μm for tracks with associated hits in each of the two layers of the silicon microvertex detector.

3 Data Sample and Monte Carlo Simulations

3.1 Data Sample and Event Selection

The analyses presented in this paper use the data sample collected between 1990 and 1994. A basic Z^0 hadronic decay selection [15], with the additional requirement of at least seven 'good' charged tracks [16], was applied. This selection has an efficiency of $(98.1 \pm 0.5)\%$, background less than 0.1%, and a flavour-bias for $\mathrm{Z}^0 \to \mathrm{b\overline{b}}$ decays of less than 0.1% [16]. After these track quality requirements, approximately 3.61 million hadronic Z^0 decay events are selected.

The identification of b-baryon decays using charge-correlated Λ-lepton combinations closely follows the selection previously employed to measure the b-baryon lifetime [10]. High-momentum electrons or muons having large transverse momentum with respect to their associated jet are first identified, then Λ baryons are reconstructed, and finally requirements are placed upon the combination of the lepton and Λ. Individual efficiencies for the selection criteria given in this section are only approximate and for illustrative purposes: the overall absolute efficiencies are not important for the lifetime analysis and details of their accurate determination for use in the product branching ratio analysis are deferred to Section 8.1.

[2] The OPAL right-handed coordinate system is defined with positive z being along the electron beam direction, and θ and ϕ being the polar and azimuthal angles, respectively.

Muons are identified by associating track segments in the outer muon detectors with tracks in the central detector. Additional requirements are made to reduce backgrounds due to misassociation and charged kaon decays [17]. The average efficiency of the muon selection is about 73% for muons with momenta greater than 3 GeV/c from semileptonic Λ_b decays. For the lifetime measurement, electrons are identified using an artificial neural net algorithm (see reference [18] for a more complete description) that is more efficient than the electron identification used in the previous lifetime analysis [10] and includes the endcap regions of the OPAL detector. The network is of a feed-forward type and was trained on simulated events to identify electrons on the basis of 12 measured quantities from the central tracking chamber and the electromagnetic calorimeters. The neural network electron selection approximately matches the efficiency and purity of the muon selection. The lifetime measurement is insensitive to systematic uncertainties in the lepton efficiency but benefits from the increased statistics of a high-efficiency selection; however, the total error of the product branching ratio strongly depends upon the uncertainty in lepton identification efficiency. The systematic error on the efficiency of the neural net electron identification algorithm is larger than the error on the efficiency of an alternative electron selection [19]. This selection covers a smaller angular range of $|\cos\theta| < 0.715$ and is based almost entirely on identifying electrons by $\mathrm{d}E/\mathrm{d}x$ measurements in the jet chamber and the ratio of the track momentum to the energy measured in the electromagnetic calorimeter. For this reason, the latter electron identification algorithm, with an efficiency of about 41% for electrons with momenta greater than 3 GeV/c from semileptonic Λ_b decays, is used for the product branching ratio result. In both cases, electron candidates identified as originating from photon conversions are rejected as outlined in Ref. [20]. Electron and muon candidates are further required to pass the track selection criteria of Ref. [10].

All charged tracks and those electromagnetic clusters not associated with a charged track are grouped into jets using the JADE algorithm with the E0 recombination scheme [21] that has the invariant mass-squared cut-off set to $x_{\min} = 49$ $(\mathrm{GeV}/c^2)^2$. In order to obtain a sample enriched in b-quark events, lepton candidates are required to have momentum greater than 3 GeV/c and transverse momentum with respect to the associated jet axis greater than 0.8 GeV/c. The lepton is included in the calculation of the jet direction.

Candidate Λ baryons are identified via the decay $\Lambda \to \mathrm{p}\pi^-$, which accounts for $(63.9 \pm 0.5)\%$ of all Λ decays [22]. Oppositely charged tracks found in the central tracking system are considered if neither track has associated hits more than 5 cm upstream from their interaction point in the x-y plane. The z components of the momenta, p_z, are recalculated under the constraint that the tracks originate from their intersection point assumed to be the Λ decay vertex. This leads to a significant improvement in the mass and momentum resolution of real Λ baryons. To reduce combinatorial backgrounds, the distance between the Λ vertex position and the beam axis is required to be greater than 5 cm. The track with the larger momentum is assumed to be the proton, and its ionization energy loss as measured in the jet chamber is required to be consistent with that of a proton, if $\mathrm{d}E/\mathrm{d}x$ information is available for that track. The measured value of $\mathrm{d}E/\mathrm{d}x$ is required to be closer to the expected value for a proton than to the prediction for a kaon. The other track, assumed to be a pion, must have a distance of closest approach to the beam axis of greater than 1 mm, to reduce combinatorial backgrounds. For Λ candidates that decay before reaching the jet chamber, it is required that in the x-y plane the primary vertex of the beam interaction point lies between the back-extrapolated trajectories of the proton and pion candidate tracks. It is further demanded that ϕ_Λ be less than 14 mrad, where ϕ_Λ is the angle in the x-y plane between the reconstructed Λ momentum vector and the line joining the primary and Λ decay vertices. To decrease the contamination due to K^0_S decays, where a pion from $\mathrm{K}^0_S \to \pi^+\pi^-$ is misidentified as a proton or antiproton, it is demanded that the invariant mass, assuming a pion mass for both particles, $m_{\pi\pi}$, not be within one standard deviation of the mass resolution of the K^0_S mass: $m_{\pi\pi} < 0.491$ GeV/c^2 or $m_{\pi\pi} > 0.503$ GeV/c^2. Reconstructed Λ baryons are required to be well contained in the sensitive part of the detector, $|\cos\theta_\Lambda| < 0.9$, where

θ_Λ is the angle between the reconstructed Λ momentum vector and the positive z axis. To reduce the contribution of Λ baryons produced from fragmentation processes, Λ candidates are required to have momentum $p_\Lambda > 4$ GeV/c. A signal region around the nominal Λ mass of 1.1157 GeV/c^2 [22] is defined by the invariant mass range $1.1078 < m_{\mathrm{p}\pi} < 1.1234$ GeV/c^2. The efficiency of the $\Lambda \to \mathrm{p}\pi$ selection depends upon momentum, and varies between a maximum of 23% for $p_\Lambda = 6$ GeV/c to 10% for high-momentum Λ baryons.

The Λ and lepton candidates are correlated through the following selection criteria. The reconstructed momentum vector of the Λ candidate is required to lie within a cone of half-angle 50° about the momentum vector of the lepton candidate. The efficiency of this cut to select a correct $\Lambda\ell$ combination from b-baryon decay is nearly 100% for lepton momentum greater than 3 GeV/c and Λ momentum greater than 4 GeV/c. Next, a cut on the invariant mass of the Λ-lepton system of $m_{\Lambda\ell} > 2.2$ GeV/c^2 is required, eliminating essentially all background from $\Lambda_c^+ \to \Lambda\ell^+\nu\mathrm{X}$. The efficiency of the invariant mass cut, after all previous cuts have been applied, is about 85%. Finally, a cut of $p_{\Lambda\ell} > 9$ GeV/c, where $p_{\Lambda\ell}$ is the magnitude of the vector sum of the Λ and lepton momenta, is imposed to reduce random combinatorial background. The efficiency of this final cut is about 97% after all other cuts have been applied.

The resulting pπ invariant mass distributions for $\Lambda\ell^-$ (right-sign) and $\Lambda\ell^+$ (wrong-sign) combinations are shown in Fig. 1, for which the neural net electron selection is used. The peak at the Λ mass in the wrong-sign distribution is due to genuine Λ baryons, mostly from fragmentation, being combined with real or misidentified leptons. A total of 874 right-sign (466 $\Lambda\mu^-$ and 408 $\Lambda\mathrm{e}^-$) and 384 wrong-sign (199 $\Lambda\mu^+$ and 185 $\Lambda\mathrm{e}^+$) Λ-lepton charge combinations are selected for the lifetime measurement. The 490 excess right-sign charge combinations are mainly attributed to b-baryon decays, compared to the 157 excess right-sign combinations of OPAL's previous lifetime analysis [10]. When the less efficient alternative electron identification algorithm is used, 268 right-sign $\Lambda\mathrm{e}^-$, and 128 wrong-sign $\Lambda\mathrm{e}^+$ combinations are selected for use in the product branching ratio analysis. As will be described in more detail later, the number of wrong-sign combinations is used as an estimate of the number of background combinations in the right-sign sample, and the distribution of the lifetime estimator in the wrong-sign sample is used to estimate the shape of the background in the right-sign sample. Note that more than one $\Lambda\ell$ combination can be associated with a particular jet.

3.2 Monte Carlo Event Samples

A number of different Monte Carlo event samples were employed to determine the efficiency of the selection, check the analyses, and estimate systematic errors. To check the analyses in the presence of general hadronic event backgrounds, approximately 2.3 million events simulating hadronic decays of the Z^0 generated by the JETSET 7.3 program [23] were used. Heavy quark fragmentation was carried out according to the Peterson *et al.* fragmentation form [24]. Additional samples enriched in b baryons were created to estimate systematic errors. Three enriched Monte Carlo samples including only the Λ_b^0 baryon were produced with JETSET 7.3. One sample, corresponding to roughly 6.5 million $\mathrm{Z}^0 \to \mathrm{b\bar{b}}$ events, was generated with $\tau_{\Lambda_\mathrm{b}} = 1.4$ ps, and two samples, each corresponding to about 2.5 million $\mathrm{Z}^0 \to \mathrm{b\bar{b}}$ events, were generated with Λ_b^0 lifetimes of 0.7 and 2.8 ps. These samples were produced using EURODEC routines [25] for Λ_c^+ decays with branching ratios adjusted to agree with measured values [26]. A form factor to describe the energy transfer from the b baryon to the c baryon in the semileptonic decay of the b baryon also needs to be included. Additional samples, which include the effects of a b-baryon decay form factor [2] calculated to first order in the inverse of the b quark mass, were also generated. In addition, to estimate the sensitivity of the measurements to the b-baryon polarization, a 'polarized' sample was created with the same form factor, assuming the longitudinal b-quark polarization of -94%, as predicted by the Standard Model, is completely transferred to the b baryon [27]. Other samples including only the Ξ_b baryon were used to assess the

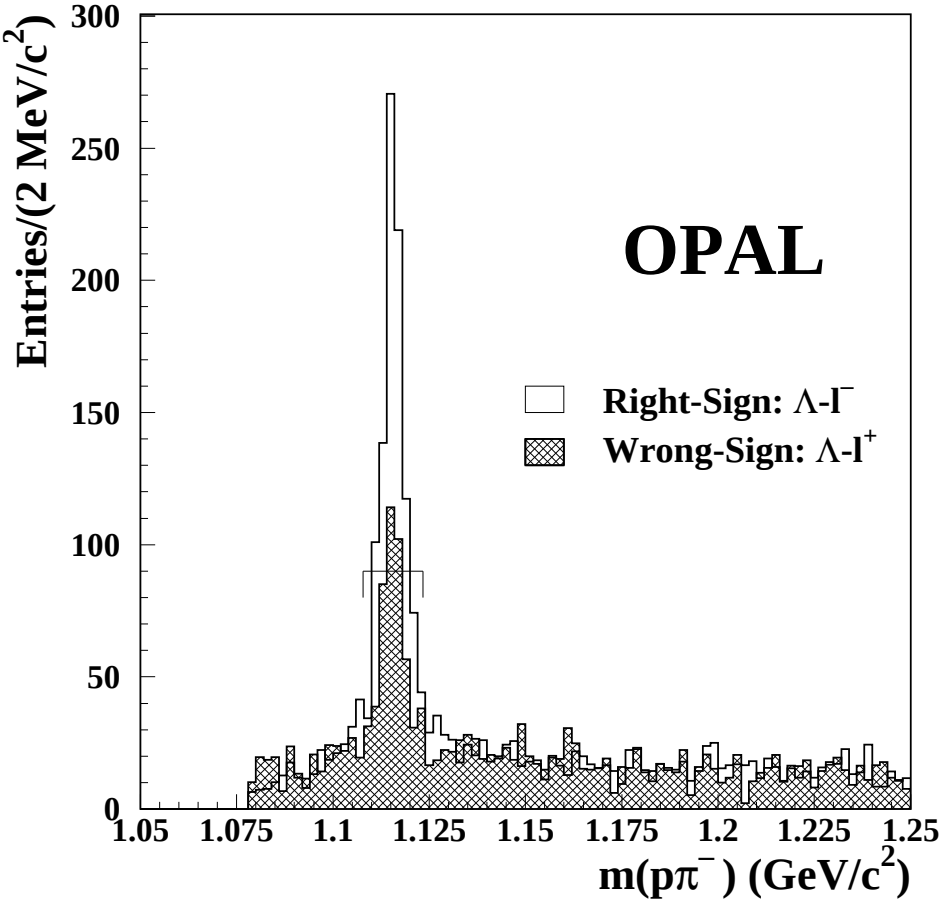

Figure 1: *Invariant mass distribution of* $p\pi$ *combinations in the* $\Lambda\ell^-$ *sample (open histogram) superimposed by* $\Lambda\ell^+$ *(shaded histogram) correlations. The signal region is shown by the bracketed range of masses. The peak at the* Λ *mass in the wrong-sign distribution is indicative of genuine* Λ *particles (though not necessarily from b-baryon decay, e.g. from fragmentation) being combined with real or fake leptons (i.e. hadrons misidentified as leptons).*

effect of different b baryons in the selected sample. All of these events were processed by a detector simulation program [28] that includes a detailed description of the detector geometry and material as well as effects of detector resolutions and efficiencies. Due to over-optimistic simulation of the detector resolution and hit-association probabilities for charged tracks, additional smearing needed to be applied to the Monte Carlo events to bring the detector resolution of tracking quantities in the r-ϕ plane into agreement with that observed in the data. The smearing method applied a multiplicative factor, $f_{d_0} = 1.4$, to the difference between the reconstructed and true track impact parameters and $f_{\phi_0} = 1.3$ to the ϕ angle measurements. Finally, when very large statistical samples were needed, a 'fast' Monte Carlo program was used that does not simulate the full detector response but rather smears four-vectors according to various empirical detector response functions.

4 Decay Length Method for Lifetime Measurement

In the first method presented in this paper, the decay length between the primary event vertex and the vertex formed by the lepton and Λ is used to estimate the flight distance of the b baryon. The fact that the lepton and the Λ do not originate from the same vertex does not introduce a significant bias in this analysis because the lifetimes of the charmed baryons are much smaller than the average b-baryon lifetime. In addition, since the difference between the charmed and the strange baryon masses is relatively small, the transverse momentum of the Λ with respect to the charmed baryon direction is also small. As a result of these two effects, the intersection of the Λ flight path and the lepton is close to the original b-baryon decay point (as discussed in Section 6).

4.1 Definition of the Decay Length

The decay length of the b baryon is estimated using the positions and error matrices of the primary vertex and the Λ-lepton vertex, subject to a directional constraint. The primary vertex is found by using the tracks in the event (excluding the candidate lepton, proton and pion tracks to avoid a systematic bias due to these tracks), as well as the averaged beam position [29], determined using large numbers of hadronic and leptonic events, as an additional constraint. The LEP beam spot has a spread of σ_x = 100–160 μm and $\sigma_y \approx 10$ μm, and the addition of the tracks in the event to determine the interaction point for each event decreases the size of the error on the production point position and on the decay length. In the directional constraint method, the decay length projection in the x-y plane is defined by the length of the line parallel to the jet containing the lepton whose endpoints minimize the χ^2 formed from the deviations of these endpoints from the primary and secondary vertices. This is converted into a three-dimensional decay length by dividing by the sine of the polar angle, with respect to the electron beam direction, of the momentum sum of the Λ and lepton.

The average decay length in the right-sign sample is 3.1 mm with an average decay length error of 500 μm due to errors on track parameters of tracks used to form the vertex. It should be noted that the major axis of the secondary vertex error ellipse tends to be aligned with the lepton direction since the lepton is more precisely measured than the Λ track parameters, due to the large lepton momentum and the long Λ lifetime that results in a large extrapolation back to the lepton track. When silicon microvertex detector tracking information is available, it is associated with about 83% of the lepton tracks but with very few of the p and π tracks used to reconstruct the Λ since it usually decays beyond the radius of the silicon microvertex detector.

Monte Carlo studies of the resolution of the decay length indicate that use of the directional constraint, rather than just the simple primary to secondary vertex distance, reduces the rms width of the residuals of the decay lengths from 3.2 mm to 2.1 mm mainly from a large reduction in the tails of the distribution. Further discussion of studies of this decay length estimator are deferred to Section 4.2.4.

4.2 Fit of the Observed Decay Length Distribution

A simultaneous fit to the decay length distributions of the right-sign and wrong-sign Λ-lepton combinations is performed to determine the average b-baryon lifetime. The modelling of the decay length distributions and the fit procedure are identical to that of the previous analysis [10] but are described here for completeness. Since the decay length distribution for the background processes is not expected to be significantly different for the right-sign and wrong-sign Λ-lepton combinations, the wrong-sign sample is used to define the background shape in the right-sign sample. The validity of this assumption

has been checked with Monte Carlo simulated events and will be discussed in the section on systematic errors.

4.2.1 Model for the Decay Length Distribution of Signal Events

For a particle with mean lifetime τ, the probability density function (PDF) for an observed proper decay time, t, with associated uncertainty, σ_t, is given by the convolution of an exponential distribution with a Gaussian distribution:

$$\mathcal{C}(\tau, t, \sigma_t) = \frac{1}{2\tau} \exp\left(\frac{\sigma_t^2}{2\tau^2} - \frac{t}{\tau}\right) \operatorname{erfc}\left(\frac{\sigma_t}{\sqrt{2}\tau} - \frac{t}{\sqrt{2}\sigma_t}\right) \ . \tag{1}$$

However, our measurements are of the decay length, l, and its uncertainty, σ_l. Therefore, we use the relation between the proper decay time and decay length,

$$t = \frac{m_{\Lambda_b}}{p_{\Lambda_b}} l \ , \tag{2}$$

where p_{Λ_b} and m_{Λ_b} are the b-baryon momentum and mass of the b baryon. To estimate the proper time, the mass of the Λ_b^0 is used. We convolute the PDF above with a distribution of b-baryon momenta, p_{Λ_b}, as described in the next section.

Estimation of the b-Baryon Momentum Spectrum

The b-baryon momentum distribution is formed from the measured Λ and lepton momenta in the data in order to be less sensitive to b-quark fragmentation uncertainties. For any event the true b-baryon momentum falls between the values of

$$p_{\Lambda\ell} = |\vec{p}_\Lambda + \vec{p}_\ell| \ \text{ and } \ p_{\Lambda_b \max} \approx \sqrt{E_{\text{beam}}^2 - m_{\Lambda_b}^2} \ . \tag{3}$$

The b-baryon enriched Monte Carlo samples with the three different lifetimes are used to determine the b-baryon momentum distribution within these limits, mapped to $y \epsilon (0,1)$. In other words, the function $g(y)$ is found, which is the PDF of the quantity y, where

$$y = \frac{p_{\Lambda_b} - p_{\Lambda\ell}}{p_{\Lambda_b \max} - p_{\Lambda\ell}} \ . \tag{4}$$

In the Monte Carlo samples, the distribution for $g(y)$ is seen not to depend strongly on $p_{\Lambda\ell}$. The b-baryon momentum distribution in the data is estimated from the convolution of the measured $p_{\Lambda\ell}$ spectrum in the data with the $g(y)$ distribution determined from the Monte Carlo. When $g(y)$ is constructed from Monte Carlo, the quantity $p_{\Lambda\ell}$ is formed from Monte Carlo reconstructed tracks to ensure that momentum resolution effects are taken into account in the formation of the estimated b-baryon momentum spectrum. A further step is taken to remove the effect of the background by subtracting the estimated effective b-baryon momentum spectrum of the wrong-sign combinations from that of the right-sign combinations. This procedure is found to reproduce the original Monte Carlo momentum distribution well and results in similar b-baryon spectra for the data and Monte Carlo samples. Figure 2 shows the $g(y)$ function determined from the enriched unpolarized b-baryon Monte Carlo samples and the resulting estimate of the b-baryon momentum spectrum for the data. The average p_{Λ_b} determined for the data is 33.9 ± 0.2 GeV/c, compared with an average of 33.7 GeV/c in the unpolarized Monte Carlo samples.

Definition of the Signal PDF

Once the b-baryon momentum spectrum is determined as described above, it is normalized and binned into 1 GeV/c bins, as shown in Fig. 2b, with the central value and content of bin i given by

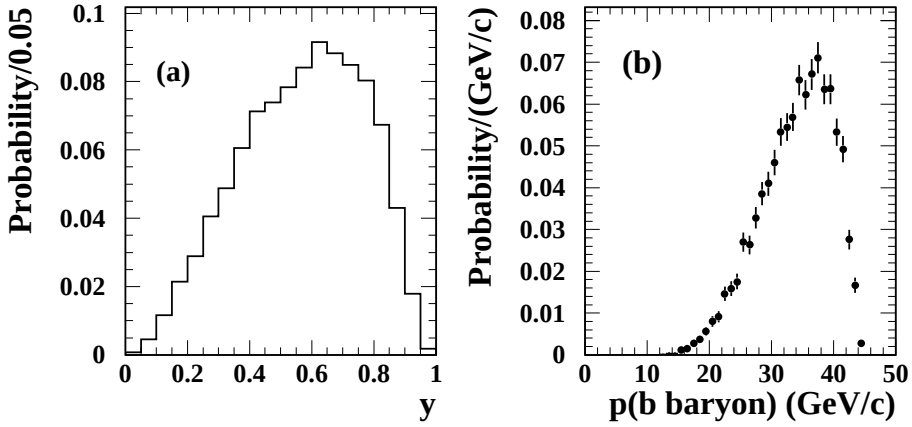

Figure 2: *a) The distribution of the variable y, as determined from the b-baryon enriched Monte Carlo samples. b) The estimate of the b-baryon momentum spectrum for the data using the procedure described in the text.*

$p^i_{\Lambda_b} = (i - \frac{1}{2})$ GeV/c and $h(p^i_{\Lambda_b})$, respectively. Then, the PDF for the decay lengths of the b-baryon signal events is found by the convolution

$$\mathcal{S}(\tau, l, \sigma_l) = \sum_{i=1}^{50} h(p^i_{\Lambda_b}) \mathcal{C}(\tau, \frac{m_{\Lambda_b}}{p^i_{\Lambda_b}} l, \frac{m_{\Lambda_b}}{p^i_{\Lambda_b}} \sigma_l) \ , \tag{5}$$

where $\mathcal{C}$ is defined previously. In order to reduce the sensitivity of the fit to the accuracy with which decay length errors are estimated and to allow for occasional mismeasurements, the signal PDF actually used is

$$\mathcal{P}_{\rm sig}(l, \sigma_l; \tau, k_1, f_2, k_2) = (1 - f_2)\, \mathcal{S}(\tau, l, k_1\sigma_l) + f_2\, \mathcal{S}(\tau, l, k_2\sigma_l) \ , \tag{6}$$

where k_1 is an error scale factor for the majority of measurements and f_2 is the fraction of events that are mismeasured with a corresponding larger scale factor k_2. This form thus describes the decay length resolution function in terms of the sum of two Gaussian distributions, which allows for resolution tails and for occasional strong underestimation of tracking parameter errors. Since the parameters k_1, f_2, and k_2 are unknown, they are allowed to vary in the lifetime fit. If the parameters f_2 and k_2 were not included, it would be necessary to restrict the range of decay lengths that are used in the fit, in order to reduce the potential bias from badly measured decay lengths. By allowing f_2 and k_2 to vary in the fit, all decay lengths are used.

4.2.2 Model for the Decay Length Distribution of Background Events

The decay length distribution for background events is parametrised in terms of an exponential and a δ-function at zero, to account for background events with and without long-lived particles, respectively, convoluted with a Gaussian distribution with standard deviation given by the measured decay length error,

$$\mathcal{B}(l, \sigma_l, L_+, b_+, b_0) = \frac{1}{b_+ + b_0}[b_+\, \mathcal{C}(L_+, l, \sigma_l) + b_0\, \mathcal{G}(l, \sigma_l)] \ , \tag{7}$$

where L_+ is a characteristic decay length of the mix of long-lived particles in the background events, and b_+ (b_0) is the fraction of events in the right-sign sample that come from background events with (without) lifetime. The function $\mathcal{C}$ was defined earlier and $\mathcal{G}(l, \sigma_l)$ is the Gaussian PDF of mean zero

and standard deviation σ_l. As in the decay length distribution for the signal, the possibility is included for a scale factor on the estimated error and also for a fraction of events to have a larger scale factor. The background PDF is thus given by

$$\mathcal{P}_{\rm back}(l,\sigma_l; L_+, b_+, b_0, \tilde{k}_1, \tilde{f}_2, \tilde{k}_2) = (1-\tilde{f}_2)\,\mathcal{B}(l, \tilde{k}_1\sigma_l, L_+, b_+, b_0) + \tilde{f}_2\,\mathcal{B}(l, \tilde{k}_2\sigma_l, L_+, b_+, b_0). \qquad (8)$$

The terms $\tilde{k}_1$, $\tilde{f}_2$, and $\tilde{k}_2$ are included in order to make the background parametrisation as general as possible. Given the variety of background sources, these parameters should not be understood as a measure of the detector resolution nor should L_+ be taken as directly indicating the lifetime of background sources since boost factors are not known.

The number of background events in the right-sign sample is taken to be equal to the observed number of events in the wrong-sign sample. Given N total Λ-lepton candidates, and the probability, p_w, that a Λ-lepton candidate has the wrong-sign correlation, the PDF for the number of background events in the right-sign sample N_w is given by the binomial PDF,

$$\mathcal{P}(N_w, N, p_w) = \frac{N!}{N_w!(N-N_w)!}\, p_w^{N_w}\,(1-p_w)^{N-N_w}\ . \qquad (9)$$

Given the definition of b_+ and b_0, the wrong-sign probability is simply $p_w = (b_+ + b_0)/(1 + b_+ + b_0)$.

4.2.3 Combined Fit of the Decay Length Distributions

The decay length PDF for the right-sign Λ-lepton combinations is described by the sum of the signal and background PDF's, $\mathcal{P}_{\rm sig}$ and $\mathcal{P}_{\rm back}$, whereas the wrong-sign combinations follow $\mathcal{P}_{\rm back}$ alone. The unbinned likelihood function is thus defined to be the product of the values of the probability density functions for all right- and wrong-sign Λ-lepton combinations multiplied by the binomial distribution given above. The log likelihood function is maximized by allowing the lifetime τ, the error scale factor parameters (k_1, f_2, k_2), and the background parameters $(L_+, b_+, b_0, \tilde{k}_1, \tilde{f}_2, \tilde{k}_2)$ to vary.

4.2.4 Corrections to the Decay Length Estimator

Tests using enriched $\Lambda_{\rm b}^0$ Monte Carlo samples indicated a systematic bias in fitted lifetimes approximately 7% below the true mean lifetimes of the events in the samples. Further investigation revealed that the bias depends roughly linearly on the quantity $|\phi_{\rm lep} - \phi_{\rm jet}|$, where $\phi_{\rm lep}$ and $\phi_{\rm jet}$ are respectively the azimuthal angles of the lepton and of the jet containing the lepton. The systematic shift was verified and its functional form with $|\phi_{\rm lep} - \phi_{\rm jet}|$ was quantified using a sample of 10^6 fast Monte Carlo events that simulates well the jet-finding directional accuracy observed in the data. Using this sample, the source of the bias was found to be a combination of the effects of errors in the determination of the jet axis, and of the directional constraint on the decay length. Large values of $|\phi_{\rm lep} - \phi_{\rm jet}|$ are sometimes spurious, resulting from an error in the determination of the jet axis due to fluctuations on the side of the true jet axis that is away from the lepton. Because the secondary vertex error ellipse is very much elongated in the direction of the lepton, the decay length is biased to shorter values. This bias of the decay length estimator was also observed and corrected for in OPAL's previous b-baryon lifetime paper [10], but was not completely understood due to insufficient Monte Carlo statistics.

Using the fitted functional form found from the fast Monte Carlo sample, the lifetime fitting procedure was modified to include a correction to the decay length for each event depending on the value of $|\phi_{\rm lep} - \phi_{\rm jet}|$. It has been checked that the distribution of this quantity shows good agreement between Monte Carlo simulated events and the data. After correction, the differences between the fitted lifetimes and mean true lifetimes are $+0.014 \pm 0.028$ ps, $+0.020 \pm 0.025$ ps, and -0.07 ± 0.09 ps for the $\Lambda_{\rm b}^0$ enriched full Monte Carlo samples generated with lifetimes of 0.7 ps, 1.4 ps, and 2.8 ps, respectively, illustrating no significant remaining bias.

4.2.5 Further Checks of the Fitting Procedure

Further checks for remaining biases in the fitting procedure and for the correct evaluation of statistical errors were performed using a simple Monte Carlo program to generate 500 data samples of on average 500 events each with decay lengths consistent with a Λ_b^0 with a lifetime of 1.4 ps. Errors on the decay lengths were increased by scale factors for different fractions of the right-sign sample, and a background distribution was generated using the model described previously and the background parameters observed in the data. In all cases, no significant additional systematic biases were observed, fitted scale factors were consistent with input scale factors, and the lifetime residuals divided by the error on the lifetime indicated a correct evaluation of statistical errors by the likelihood fit.

Since the overall fitting model is not linear in the fit parameters, and a maximum log likelihood fit instead of least-squares is performed, a goodness-of-fit test using ordinary χ^2 measures, with numbers of degrees of freedom given by the number of bins minus the number of fit parameters, is not valid. Instead, the form of the "χ^2" distribution of weighted deviations of fitted versus input parameters was determined using the above simple Monte Carlo samples. Splitting the right-sign decay length sample between -1 and 2 cm into 11 bins and the wrong-sign sample into 5 bins, the "χ^2" variable is observed to follow that of ordinary χ^2 distributions with 11 and 5 degrees of freedom, respectively. This allows an evaluation of the quality of the fit to the data given below.

The complete analysis applied to a sample of 2.3 million fully simulated hadronic Monte Carlo events results in a sample of 767 right-sign and 281 wrong-sign combinations. Note that the fraction of excess events obtained in the Monte Carlo sample is larger than in the data because the value of $f(\mathrm{b} \to \Lambda_\mathrm{b}) \cdot BR(\Lambda_\mathrm{b} \to \Lambda \ell^- \bar{\nu} X)$ is larger in the Monte Carlo than the value observed in the data (see Section 8). The fitted lifetime of $1.32^{+0.12}_{-0.11}$ ps is consistent with the true mean lifetime observed in the particular selected sample of 1.37 ps.

4.3 Result of the Decay Length Lifetime Fit to the Data

The result of the fit to the full data sample, shown in Fig. 3, gives $\tau = 1.10 \pm 0.12$ ps. The χ^2 of the fit, as defined in Section 4.2.5, is 13.2 and 1.6 for the right-sign and wrong-sign candidates for an estimated 11 and 5 degrees of freedom, respectively. The values of all the parameters of the fit are shown in Table 1.

τ (ps)	k_1	f_2	k_2	L_+ (cm)
1.10 ± 0.12	1.34 ± 0.26	0.02 ± 0.02	26.9 ± 8.7	0.24 ± 0.02
b_+	b_0	$\tilde{k}_1$	$\tilde{f}_2$	$\tilde{k}_2$
0.32 ± 0.03	0.13 ± 0.02	1.27 ± 0.13	0.21 ± 0.03	11.8 ± 1.2

Table 1: *The model parameters found in the decay length fit to the data.*

The likelihood function is found to be well-behaved and almost parabolic. By scanning across fixed lifetime values below and above the central value and allowing the other parameters to vary to maximize the likelihood, the 2 and 3 standard deviation points are found to occur at $(-0.23, +0.25)$ps and $(-0.35, +0.39)$ps away from the central value of 1.10 ps, respectively.

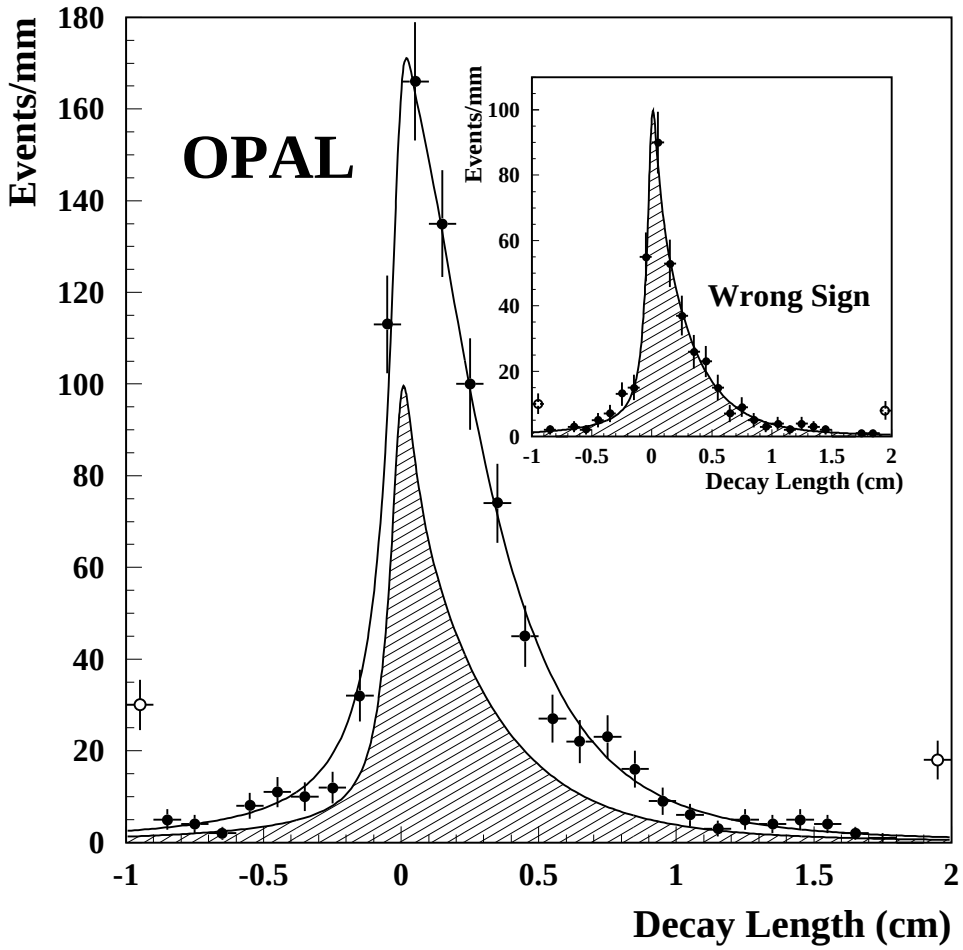

Figure 3: *The distribution of measured decay lengths, shown with the result of the fit. The fitted distribution of the background in the right-sign sample is shown by the shaded area. The inset figure shows the distribution for the wrong-sign candidates. The underflow and overflow entries, shown in the first and last bins, have large decay length errors.*

5 Impact Parameter Method for Lifetime Measurement

5.1 Fit of the Observed Impact Parameter Distribution

In this method, the average lifetime of b baryons is determined from a maximum likelihood fit to the impact parameter distribution of the leptons from Λ_b decays using a method similar to that used by OPAL to determine the average inclusive b-hadron lifetime [4]. Only those lepton tracks that have at least one hit in the silicon microvertex detector were used since the error on the impact parameter measurement benefits from this added high-precision tracking information. After this requirement a data sample of 604 right-sign and 248 wrong-sign Λ-lepton combinations remains.

The impact parameter, d_0, is defined as the closest distance in the plane transverse to the beam axis between the lepton track and the primary vertex. The primary vertex is fitted for each event separately as described for the decay length method. The sign of the impact parameter is defined as positive if the angle in the x-y plane between the vector from the primary vertex to the point of closest approach of the track and the axis of the jet including the lepton is less than 90°, otherwise it is defined as negative.

To obtain a lifetime using the impact parameter distribution, a model for the expected distribution is necessary. This model can be divided into two parts. The first describes the expected distribution of signal events and the second part describes the background. Since the impact parameter distribution obtained from background events is expected to be independent of the sign of the Λ-lepton correlation, the wrong-sign sample is used to define the background shape in the right-sign sample. A simultaneous fit to the impact parameter distributions of right-sign and wrong-sign Λ-lepton combinations is then performed to determine the average b-baryon lifetime.

5.1.1 Model for the Signal Events

The observed impact parameter distribution of leptons from true b-baryon decays is determined both by the average b-baryon lifetime and decay kinematics, and by detector resolution. In this analysis, the probability density function $\mathcal{P}_{\rm sig}$ for the impact parameter distribution of the signal events is described by a convolution of the distribution expected from the underlying physics processes $\mathcal{S}_{\rm phys}$ with a detector resolution function that is fitted simultaneously with the lifetime. The resolution function describes the impact parameter resolution of the lepton track.

The underlying physics distribution is the impact parameter distribution that would be obtained from a detector with perfect impact parameter resolution. The $\mathcal{S}_{\rm phys}$ distributions are determined using samples of approximately 400 000 unpolarized $\mathrm{Z} \to \Lambda_{\rm b}^0 \to \Lambda\ell$ events. The events are processed using the fast simulation of the OPAL detector. The impact parameters are taken directly from the generated four-vector information before the detector simulation, but only lepton tracks from events that pass all kinematical and geometrical Λ-lepton selection criteria are entered into the distribution. Since the detector-related Λ identification variables have no influence on the underlying physics distribution, no efficiency corrections for these variables were applied. Lepton identification criteria are not imposed because the fast Monte Carlo simulation gives an inadequate description of the identification variables. Instead, the lepton impact parameters are weighted using tables of lepton identification efficiencies as functions of lepton momentum and transverse momentum with respect to the associated jet obtained from the full Monte Carlo simulation. The impact parameters are calculated relative to the true primary vertex, and their signs are determined using the jet axis reconstructed from charged tracks and unassociated electromagnetic clusters obtained after the detector simulation. This procedure is necessary because the sign of the impact parameters is determined by the other particles in the jet whereas the resolution function applies only to the lepton candidate track and therefore cannot account for signing errors due to imprecise estimates of the $\Lambda_{\rm b}^0$ direction. The distribution is parametrised using a sum of exponential functions in order to facilitate an analytic convolution with the resolution function. Three exponential functions describing the negative part of the distribution and four exponential functions describing the positive part of the distribution were found to provide a good description. The underlying physics distribution given as a function of the "scaled" impact parameter expressed in terms of the impact parameter divided by the product of the speed of light and the average generated lifetime of the $\Lambda_{\rm b}^0$ sample of $\tau = 1.5$ ps, is shown in Fig. 4 along with the result of the fit.

The resolution function is parametrised using a Gaussian, $\mathcal{G}$, of mean zero. The uncertainty of the impact parameter is taken as the sum in quadrature of the error from the track fit, which includes contributions due to multiple scattering, and the uncertainty from the primary vertex error ellipse:

$$\sigma^2 = (\sigma_{\rm track}^2 + \sigma_{\rm prim}^2). \tag{10}$$

The actual width of the Gaussian $\mathcal{G}$ used in the fit is $a \cdot \sigma$. The parameter a is introduced to reduce the sensitivity of the fitted lifetime to systematic mis-estimation of the errors on the impact parameter, and to deviations of the real background from the background model described later. Thus the probability

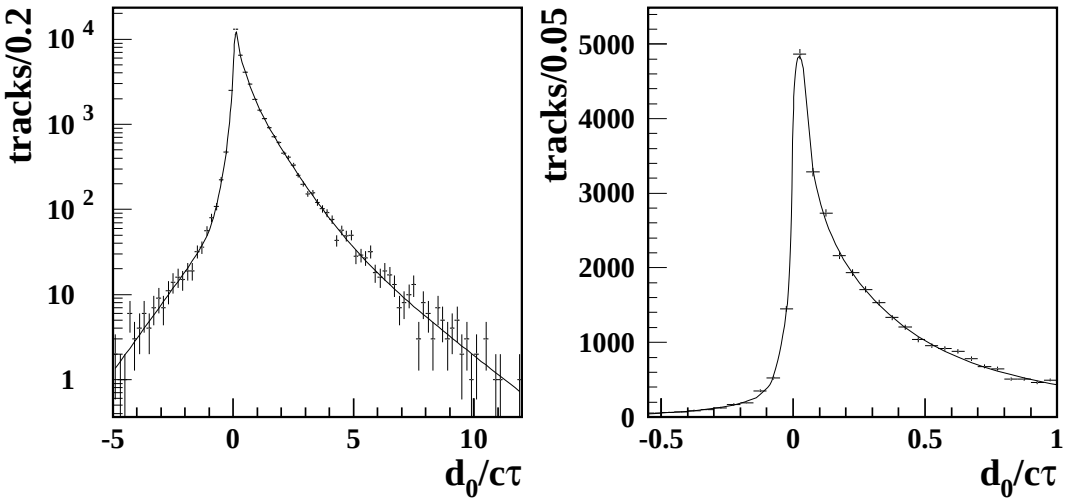

Figure 4: *The underlying physics distribution for the "scaled" impact parameter for leptons from unpolarized Λ_b^0 decays. The left plot shows the full range of the distribution whereas the right plot shows the central part. The curves are the result of the fit using a sum of exponentials as described in the text. The χ^2 of the fit is 1.01/d.o.f.*

density function for the impact parameter distribution of leptons from Λ_b decays used in this analysis is the convolution of $\mathcal{S}_{\rm phys}(d_0;\tau)$ with $\mathcal{G}(d_0, a\sigma)$,

$$\mathcal{P}_{\rm sig}(d_0,\sigma;\tau,a) = \mathcal{S}_{\rm phys}(d_0;\tau)\otimes\mathcal{G}(d_0,a\sigma), \tag{11}$$

where the parameters τ and a are allowed to vary in the fit.

5.1.2 Model for the Impact Parameter Distribution of Background Events

The impact parameter distribution of background events is expected come from tracks that originate at the primary vertex and to tracks that arise from secondary decays of particles with a non-zero lifetime. The underlying physics distributions of tracks from the primary vertex can be parametrised as a δ-function at zero. The impact parameters from tracks from secondary decays form an impact parameter distribution that can be expressed in terms of a sum of exponentials. These exponentials parametrise the underlying physics processes and particle compositions. Three exponentials have been chosen: one to describe the negative impact parameters and two to describe the positive impact parameters. This parametrisation of the underlying physics distributions is convoluted with a Gaussian with errors given by the measured errors of the impact parameters. The probability density function for the background can be written as

$$\begin{aligned}\mathcal{P}_{\rm back}(d_0,\sigma;A_1^+,b_1^+,A_2^+,b_2^+,A^-,b^-,b^0) &= \frac{1}{b^0+b_1^++b_2^++b^-}[b^0\mathcal{G}(d_0,\sigma)+b_1^+\mathcal{C}(A_1^+,d_0,\sigma)+\\ &\quad b_2^+\mathcal{C}(A_2^+,d_0,\sigma)+b^-\mathcal{C}(A^-,d_0,\sigma)],\end{aligned}$$

where $\mathcal{C}(A,d_0,\sigma)$ is the convolution of an exponential with a Gaussian $\mathcal{G}(d_0,\sigma)$ of mean zero and standard deviation σ, b^0 is the fraction of tracks from the primary vertex and b_1^+, b_2^+, b^- are the

fractions of tracks in the right-sign sample from secondary decays that can be described by convolutions of positive or negative exponentials with a Gaussian, respectively. The parameters A_1^+, A_2^+ and A^- are the corresponding decay constants in the exponential functions. Since the composition and shape of the background in the right-sign sample are not known a priori, all fractions and decay constants are allowed to vary in the fit.

As in the decay length method, the number of background events in the right-sign sample is given by a binomial distribution based on the number of observed events in the wrong-sign sample, where in this case the wrong-sign or background probability is $p_\omega = (b^0+b_1^++b_2^++b^-)/(1+b^0+b_1^++b_2^++b^-)$. As previously, the probability density function for leptons in the right-sign sample is described by the sum of the signal and background PDF's, $\mathcal{P}_{\rm sig}$ and $\mathcal{P}_{\rm back}$, whereas leptons in the wrong-sign sample follow $\mathcal{P}_{\rm back}$ alone. The log likelihood function is maximized by allowing the lifetime τ and the parameters $(a, b_1^+, b_2^+, b^-, b^0, A_1^+, A_2^+, A^-)$ to vary.

5.1.3 Checks of the Fitting Procedure with Monte Carlo

The $\Lambda_{\rm b}^0$ Monte Carlo samples generated with different lifetimes were used to check the probability density function $\mathcal{P}_{\rm sig}$ for the signal events. The Monte Carlo samples were split into subsamples of approximately 350 events each. The fitted lifetimes show good agreement with the average true lifetime of events in the specific subsample after the selection. The average differences between the fitted and generated lifetimes are -0.006 ± 0.033 ps, 0.006 ± 0.036 ps and 0.014 ± 0.144 ps for the Monte Carlo samples generated with lifetimes of 0.7 ps, 1.4 ps and 2.8 ps, respectively.

To check that no additional bias exists in the fitting procedure when background is included, and that the statistical error of the fit is accurate, a simple Monte Carlo program was used to produce 200 samples of on average 600 events each, with impact parameters following a distribution arising from semileptonically decaying $\Lambda_{\rm b}^0$ baryons with a lifetime of 1.4 ps. The majority of impact parameter values were smeared in each sample to increase the errors of the impact parameters by a scale factor of 1.2 in order to reproduce more accurately the impact parameter tracking error distribution observed in the data. In addition, a fraction of approximately 10% of impact parameters in each sample were smeared using a scale factor of 5.0 to simulate more realistically pattern recognition and tracking mistakes. For each $\Lambda_{\rm b}^0$ sample, a background distribution was generated according to the model described above with the background parameters $b_1^+, b_2^+, b^-, b^0, A_1^+, A_2^+, A^-$ set to the same values as found from data.

The average difference between the fitted lifetimes and the generated lifetimes is 0.008 ± 0.013 ps, indicating no bias when the full fitting procedure including background is used. The distribution of lifetime residuals divided by errors is described by a Gaussian of width 1.07 ± 0.10, indicating that the statistical error is accurate. The average fitted value of the parameter a is 1.80 with an rms width of 0.38, and the correlation coefficient between the fitted lifetime and this parameter using the simple Monte Carlo is -0.121. This demonstrates that the variable a cannot be interpreted as a scale factor of the resolution.

As a consistency check, in the JETSET five-flavour hadronic Monte Carlo events a sample of 615 right-sign and 211 wrong-sign events was subjected to the requirement that the lepton has at least one hit in the silicon detector. The true mean lifetime of the sample after the selection is 1.37 ps. The fitted lifetime $\tau = 1.40^{+0.14}_{-0.13}$ ps is consistent with both the input lifetime of 1.4 ps and the true lifetime of the sample.

5.2 Result of the Impact Parameter Lifetime Fit to the Data

The result of the fit to the selected events in the data using an underlying physics function modelled using unpolarized Λ_b^0 decays is shown in Fig. 5. The fit gives a lifetime value of $\tau = 1.15^{+0.14}_{-0.13}$ ps. The χ^2 of the fit is 24.2/23 d.o.f. The values of the other parameters in the fit are shown in Table 2.

τ(ps)	a	$A_1^+(\mathrm{cm}^{-1})$	$A_2^+(\mathrm{cm}^{-1})$	$A^-(\mathrm{cm}^{-1})$
$1.15^{+0.14}_{-0.13}$	2.5 ± 0.3	$89. \pm 28.$	$17. \pm 3.$	$20. \pm 4.$

b^0	b_1^+	b_2^+	b^-
0.07 ± 0.02	0.16 ± 0.03	0.13 ± 0.03	0.03 ± 0.01

Table 2: *The parameter values found in the impact parameter fit to the data.*

The likelihood function is found to be approximately parabolic. By fixing the lifetime at various points and allowing the fit to maximize the likelihood, the 1, 2 and 3 standard deviation points are found to occur at $(-0.13, +0.14)$, $(-0.28, +0.30)$ and $(-0.40, +0.50)$ps away from the central value of 1.15 ps.

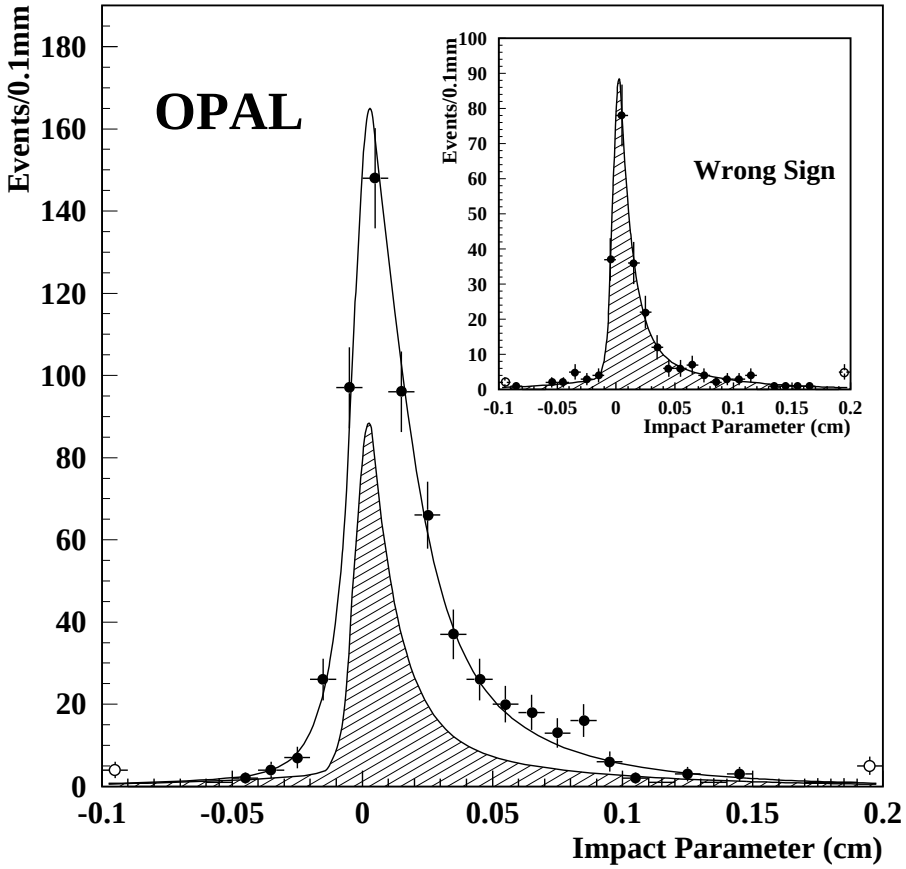

Figure 5: *The distribution of impact parameters is shown, along with the result of the fit. The fitted distribution of the background in the right-sign sample is shown by the shaded area. The inset figure shows the distribution for the wrong-sign candidates. The underflow and overflow entries are shown in the first and last bins.*

6 Estimates of Systematic Uncertainties on Lifetime Results

The quoted statistical errors for both lifetime results already account for some systematic uncertainties because of the free parameters that are allowed to vary in the fits. For example, statistical uncertainties in the resolutions as well as statistical uncertainties in both the estimated normalization and shape of the background in the right-sign sample are already included. When all the background model parameters are fixed to their fitted values and the fits repeated, the central values of the lifetimes remain the same as expected, but for both lifetime methods, the statistical error decreases by 0.020 ps, corresponding to an additional error of about 0.07 ps added in quadrature. The systematic uncertainties and biases due to additional effects that were considered for the two lifetime methods are discussed below and shown in Table 3.

Source	Systematic Error (ps)	
	Decay Length	Impact Parameter
Primary vertex estimate	± 0.01	± 0.02
Background shape and normalization	± 0.03	± 0.04
b-baryon decay model	± 0.02	± 0.03
b-baryon polarization	$+0.03 \pm 0.03$	$+0.065 \pm 0.065$
Ξ_b content (b-baryon mass)	$+0.02 \pm 0.02$	± 0.01
Decay length estimator	± 0.03	–
b-baryon momentum estimate method	± 0.01	–
b fragmentation	–	± 0.01
Physics distribution statistics	–	± 0.04
Resolution function	–	± 0.01
Lepton efficiency	–	± 0.01
Silicon det. alignment and calib.	–	± 0.01
Total	$+0.05 \pm 0.06$	$+0.065 \pm 0.10$

Table 3: *Table of systematic uncertainties and corrections for the decay length and impact parameter methods.*

6.1 Primary Vertex Estimate

The primary vertex is determined using tracks in the event, excluding the lepton and tracks forming the Λ, and including the constraint of the average LEP beam spot measured over the span of several hundred events. To test the sensitivity of the lifetime measurements to the position of the primary vertex, the centroid of the LEP beam spot is moved in the x direction by 50 μm and in the y direction by 20 μm as well as increasing the beam size by a factor of two in each dimension. The centroid of the beam spot is known to typical precisions of 25 μm in the x direction and 10 μm in the y direction, and the width of the beam spot is known to better than 10 μm in both directions. The maximum lifetime shift observed is 0.01 ps for the decay length method and 0.007 ps for the impact parameter method.

In the data and the Monte Carlo, lifetime fits were also performed without including any prior knowledge of the average interaction point in the event. This results in a larger error ellipse for the primary vertex and a difference in fitted lifetimes of 0.025 ps for the decay length method. Knowledge of the average interaction point is used to reduce this bias, and any residual bias was investigated by finding the difference in position of the fitted interaction point projected along the direction of the jet axis between the cases of including and not including tracks in the event. A very small shift of

5 ± 1 μm was observed in the direction away from the hemisphere containing the Λ-lepton combination, presumably due to b-hadron secondary vertex tracks on the other side tending to pull the primary vertex. This 5 μm gives a lifetime difference of much less than 0.01 ps, and a systematic error of 0.01 ps for the decay length method is taken due to the uncertainty in the determination of the primary vertex.

To investigate a possible bias of the impact parameter method lifetime due to the use of the fitted primary vertex, the impact parameter with respect to the fitted vertex was compared with the impact parameter calculated with respect to the average interaction point. The impact parameter with respect to the average interaction point turns out to be on average 5 ± 3 μm smaller. Shifting each impact parameter by $-5\,\mu$m results in a lifetime that is 0.02 ps smaller. The uncertainties of the primary vertex estimate position and size discussed above for the impact parameter method are added in quadrature to determine a systematic error of 0.02 ps.

6.2 Background Normalization and Shape

In addition to statistical fluctuations of the normalization and shape of the wrong-sign background, which are already included in the quoted statistical errors, systematic effects are also considered. It is assumed that the background enters the right-sign and wrong-sign distributions with equal probability. Using Monte Carlo hadronic event samples, the decay length and impact parameter distributions of the right- and wrong-sign background samples are found to be statistically consistent, and also give statistically consistent results for fitted lifetimes if their roles are reversed in the fit method.

As will be discussed in Section 8.2, the background of fragmentation Λ baryons combined with leptons from b-baryon decays preferentially populates the wrong-sign sample. Monte Carlo studies used for the product branching ratio determination indicate that $(12 \pm 2)\%$ of the wrong-sign combinations are due to b-baryon decays. Repeating the lifetime analysis after scaling the background in the right-sign sample by 0.88 ± 0.02 results in lifetime shifts of only 0.001 ps for the decay length method, and 0.003 ps for the impact parameter method, which are ignored as systematic errors. Another check, in which the fit to the data is made by fixing the model parameters of the background shape and allowing only its normalization to vary, gives similar insignificant shifts.

Although the background considered above is seen to contribute unequally to the right- and wrong-sign samples, the effect on the lifetime measurements is negligible since the lifetime distributions are very close to those of the signals. As shown in the study of backgrounds in Section 8.2, the effects of related background asymmetries due to fragmentation Λ baryons, when combined with leptons from B meson decays which preferentially populate the right-sign sample, are small and can be ignored. The same is true for the predicted small fraction of background exclusive decay channels discussed in that section. The worst case is the background due to the exclusive decay channel $\Lambda_c^+ \to \Lambda \ell^+ \nu$ that enters only the wrong-sign sample at the level of $(2.5 \pm 0.3)\%$ as estimated by Monte Carlo simulations. By performing lifetime fits on Monte Carlo samples with and without this background, lifetime differences of 0.005 ps or less are found.

Of more concern is the background due to fragmentation Λ baryons that combine with leptons from c-meson decays, which enter the wrong-sign sample more often. These events have a significantly different decay length distribution, but the maximum prediction of an excess of these events in the wrong-sign sample is 24 events for the decay length method. As a further check, the data are divided into two roughly equally sized and independent samples with $p_\Lambda > 6.6$ GeV/c and $p_\Lambda < 6.6$ GeV/c, in order to deplete and enrich, respectively, the contribution from fragmentation Λ baryons. The wrong-sign samples in the low momentum range show longer tails in both the decay length and impact parameter distributions compared with the wrong-sign samples in the high momentum range; however, the shapes of the wrong-sign samples are consistent within statistical fluctuations. Each data sample was fitted twice using the wrong-sign samples of both high and low momentum intervals to

study the effects of the different shapes of the wrong-sign distributions. Fitting the right-sign samples of both momentum ranges with the wrong-sign sample of the low Λ momentum results in shorter lifetimes compared to the results of the fits to the right-sign samples using the wrong-sign sample of high p_Λ. Since the correct shape of the background in the data is not known exactly, the maximum differences of 0.03 ps for the decay length method and 0.04 ps for the impact parameter method are taken as systematic errors.

6.3 b-Baryon Decay Model

The enriched Monte Carlo events used to find the function $g(y)$ for the decay length method and the underlying physics distributions for the impact parameter method employed theoretical predictions [2] for a form factor to describe the energy transfer from the b baryon to the c baryon in the semileptonic decay of the b baryon. No measurements have been made of the form factor, so differences in fitted lifetimes observed between the functions used for the central lifetime value, and those obtained using an alternate theoretical form factor [27], and those using no form factor, were used to estimate a systematic error due to this source. The maximum lifetime differences observed are 0.018 ps for the decay length method and 0.03 ps for the impact parameter method. These variations should also encompass the effects of some fraction of decays proceeding through higher mass charm baryon states. In addition, the decay branching ratios for Λ_b and Λ_c^+ in the EURODEC [25] decay tables are varied, giving maximum lifetime shifts of 0.015 ps. Combining errors in quadrature, a systematic error of 0.02 ps is taken for the decay length method and 0.03 ps for the impact parameter method to account for uncertainties in the b-baryon decay model.

6.4 b-Baryon Polarization

The $g(y)$ function and underlying impact parameter physics distributions were determined using a sample of unpolarized Λ_b^0 baryons. However, since it is expected that the Λ_b baryons produced in Z^0 decays are polarized to some degree [27], separate underlying physics distributions are found for a longitudinal polarization of 0% and the maximum possible polarization of -94% as expected for b quarks in the Standard Model. When the polarized Λ_b^0 sample is used to define the $g(y)$ function and underlying physics distributions, the lifetime measurements increase by 0.06 ps for the decay length method and 0.13 ps for the impact parameter method. Leptons from polarized Λ_b-decays are preferentially emitted along the Λ_b flight direction. This leads to smaller angles between the lepton and the Λ_b and therefore to smaller expected impact parameters. The decay length is less sensitive to these changes. Since there is no published measurement of b-baryon polarization, systematic corrections of $+0.03 \pm 0.03$ ps for the decay length method and $+0.065 \pm 0.065$ ps for the impact parameter method are applied to the data to encompass the full range of possible polarizations. This range would also cover polarization effects of Ξ_b baryons and other higher spin states, plus residual polarization transfer to the Λ_c and Λ.

6.5 b-Baryon Mass and Ξ_b Content

The mass of the b baryon is used in the decay length analysis to convert from decay times to decay lengths. The JETSET default Λ_b^0 mass of 5.62 GeV/c^2 is used in the analysis, and most of the enriched Monte Carlo samples contain only Λ_b^0 decays and no other b baryons. Monte Carlo studies with samples containing a mixture of b baryons show that the analysis selects a mixture of b baryons dominated by the Λ_b^0. Inputs to the model in the JETSET Monte Carlo from low-energy baryon measurements, assumed to be valid for heavier baryons at higher energies, result in the prediction that 12% of b baryons before the selection may be Ξ_b baryons. This result is consistent with first measurements of this rate [30]. These baryons are expected [31] to have masses 0.2–0.3 GeV/c^2 larger

than the Λ_b^0 mass, and the fraction is chosen to vary between the values of 0% and 24%. The overall b-baryon mass is therefore taken to be 5.7 ± 0.1 GeV/c^2. By repeating the decay length analysis using masses within this range, a systematic correction of $+0.02 \pm 0.02$ ps is assigned to the measurements to account for uncertainties in the b-baryon mass. This shift is verified by fitting to an enriched Monte Carlo sample containing only Ξ_b decays. Similarly, to estimate the effect of leptons coming from Ξ_b on the lifetime found using the impact parameter method, the fraction of Ξ_b in the sample used to determine the underlying physics distribution was varied in the above range and the resulting lifetime difference of 0.01 ps is used as a systematic error. The impact parameter method is much less sensitive to the value of the b baryon mass.

6.6 Bias of Decay Length Estimator

For the decay length method, the enriched Λ_b full Monte Carlo samples were first used to assess any systematic bias on the lifetime due to the selection criteria. From the difference between the true mean lifetime of the signal in the entire sample and the true mean lifetime after Λ-lepton combination selection, a negligible difference of less than 0.004 ps is observed.

The effect of the non-zero Λ_c^+ lifetime on the decay length measurement was assessed using samples of 250 000 fast Monte Carlo events of the signal channel with the Λ_c^+ lifetime ($\tau_{\Lambda_c} = 0.200^{+0.011}_{-0.010}$ ps [22]) varied within its errors. The maximum variation in fitted lifetime between this sample and a sample with zero Λ_c^+ lifetime was 0.005 ps. The presence of the Λ_c^+ therefore does not result in a significant bias.

The correction of the bias that depends upon $|\phi_{\rm lep} - \phi_{\rm jet}|$, when the jet axis of the jet containing the lepton is used as a directional constraint, has already been discussed in Section 4.2.4 and is corrected for within the fitting procedure. This correction amounts to 6% of the lifetime, or about 0.07 ps in this case. The uncertainty in this correction due to statistical errors in the determination of the parameters of its functional form in the fast Monte Carlo is 0.015 ps. Two other decay length estimators are considered to check if the Monte Carlo samples reproduce the observed biases in the data and provide an adequate simulation of the effect. The first of these alternate decay length estimators uses the direction of the momentum sum of the Λ and lepton as a directional constraint instead of the jet axis and results in an observed bias in the Monte Carlo as high as 17%, while the second uses no directional constraint and is found to have little bias, but significantly poorer resolution. In both cases, the Monte Carlo fits reproduce the differences between the different lifetime estimators observed in the data to within 0.03 ps. The systematic error assigned to the decay length estimate is therefore taken to be the addition in quadrature of the errors above, which is 0.03 ps.

6.7 b-Baryon Momentum Estimate Method

The method used to estimate the b-baryon momentum for the decay length method was checked using full Monte Carlo samples by comparing the lifetime found using the true p_{Λ_b} distribution in the convolution to obtain decay times with the lifetime found using the reconstructed distribution of p_{Λ_b} using $g(y)$. The observed lifetime difference of 0.01 ps is assessed as the systematic error due to the method to estimate the b-baryon momentum. In the enriched Λ_b^0 samples, the true value of $\langle p_{\Lambda_b} \rangle$ is 33.7 GeV/c, while the reconstructed value of $\langle p_{\Lambda_b} \rangle$ in the same events used to determine $g(y)$ is found to be 34.1 GeV/c.

6.8 b Fragmentation

The fragmentation parameter ϵ_b in the Peterson fragmentation scheme [24] was varied between 0.0025 and 0.0095 [19]. A maximum variation of the lifetime of 0.01 ps was found for the impact parameter method and assigned as a systematic error due to this source. No significant lifetime shift was observed

for the decay length method since the technique used to estimate the b-baryon momentum uses observed track momentum and follows the changing momentum spectrum due to different fragmentation variables.

6.9 Underlying Physics Distribution Statistics

Each parameter of the functions describing the $\Lambda_b^0 \to \ell$ underlying physics distribution for the impact parameter method was varied by its statistical uncertainty. The maximum variation of 0.04 ps was conservatively taken as a systematic error.

6.10 Resolution Function

In the impact parameter analysis, results from the simple Monte Carlo study indicate that the fitted value of the parameter a increases when background is included in the fit. To study the effect of the parameter a on the lifetime, a second parameter a_2 for a fraction f_2 of events was introduced. The fitted values are $a = 2.4 \pm 0.4$, $a_2 = 7.2 \pm 5.4$ and $f_2 = 0.08 \pm 0.15$. These parameters are poorly measured and highly correlated indicating that the fit is unable to separate the two components of errors. However, the observed difference in the fitted lifetime of 0.01 ps is included as an estimate of the systematic error due to inadequate modelling of the detector resolution.

6.11 Lepton Efficiency

To study the effect of the lepton efficiency tables on the lifetime determined using the impact parameter method, an alternate underlying physics distribution was used in which electrons and muons were taken according to their relative fraction as seen in the data, assuming that the efficiency is flat over the entire p and p_t range. The difference in the fitted lifetime of 0.01 ps using this alternate physics distribution is included as a systematic error.

6.12 Silicon Microvertex Detector Calibration and Alignment

The effect of silicon microvertex detector misalignment and calibration uncertainties was studied using the measured distribution of the apparent separation at the interaction point of the two tracks in muon-pair events. The signing convention used is expected to result in a symmetric distribution centred at zero. Instead an average shift of $3.4 \pm 0.5\ \mu$m was found due to a combination of the radial position uncertainty of the ladders of the silicon detector, drift chamber calibration uncertainties and remnant shifts or rotations of one detector with respect to another. A study of this effect indicates that this translates into a shift of lifetime of 0.01 ps, which is taken as a systematic error for the impact parameter method. For the decay length method, since the Λ typically has a long decay length, it is usually reconstructed outside the sensitive volume of the silicon microvertex detector and the vertex chamber, making the decay length much less sensitive to these alignment and calibration uncertainties. This has been checked in Monte Carlo simulations. Because the major axis of the $\Lambda\ell$ vertex error ellipse is nearly aligned with the lepton direction, the decay length error is dominated by the uncertainty of the projection of the Λ.

6.13 Consistency Checks

Further checks were performed to search for other systematic effects. The data were divided into two roughly equally-sized samples using various criteria, and the lifetimes for each sample were determined. Separation into high and low lepton momentum, high and low transverse momentum with respect to

the jet, positive and negative lepton electric charge, horizontal and vertical quadrants, high and low Λ momentum, data collected in 1990–1993 and data collected in 1994, Λ-electron and Λ-muon samples, and two bins according to the $\cos\theta$ of the lepton track were all investigated. The lifetime results between the pairs of statistically-independent subsamples were consistent.

7 Combination of Lifetime Results

After applying the above systematic corrections to the fitted lifetime values, the decay length method gives a value for the average lifetime of b baryons of:

$$\tau = 1.15 \pm 0.12 \pm 0.06 \text{ ps},$$

where the first error is statistical and the second is systematic.

The impact parameter method gives

$$\tau = 1.21^{+0.15}_{-0.13} \pm 0.10 \text{ ps}.$$

Since in both cases the statistical fit errors are relative rather than absolute, they are adjusted appropriately when the systematic corrections are applied.

Although it is clear that the lifetime result using the decay length method is strongly correlated with the result of the impact parameter method, some gains can be made in the reduction of the total error when the two results are combined. Geometry demands that in some event topologies there can be a zero impact parameter but a non-zero decay length. On the other hand, the impact parameter method is better able to exploit the high precision measurements of the silicon microvertex detector. The two separate methods therefore provide a valuable cross check.

7.1 Statistical Correlation between Methods

The statistical correlation coefficient between the methods is found using various Monte Carlo event samples. The enriched signal Monte Carlo sample with $\tau = 1.4$ ps is split into subsamples of about 500 events each. The lifetime is fit using each of the two methods and a strong correlation is observed. The 0.7 ps and 2.8 ps enriched Monte Carlo samples are also employed. After checking that the impact parameter method applied to the enriched Monte Carlo samples gives results essentially proportional to the mean impact parameter, a sample of 500 000 fast Monte Carlo events was also used to calculate and check the correlation coefficient with high precision.

When the same Λ-lepton combinations are considered for each method, the statistical correlation coefficient is 0.71. About 83% of selected leptons have at least one silicon microvertex detector hit (as required by the impact parameter method) and the silicon microvertex detector was not operational in 1990, early in the 1991 run, and in the last 20% of the 1994 run. The decay length method considers these events, which are not used in the impact parameter method. The 604 right-sign and 248 wrong-sign combinations considered by the impact parameter method are a subset of the 874 right-sign and 384 wrong-sign combinations considered by the decay length method. A simulation of the wrong-sign background shape for each of the methods was also included in the fast Monte Carlo study, with the result that background dilutes the correlation coefficient very little because when the same wrong-sign combinations are considered by each method, the background shapes are also correlated. The overall coefficient of statistical correlation is found to be 0.56.

7.2 Calculation of Errors in Combination

The weight given to each of the two measurements is such that the total relative error σ/τ (statistical plus systematic error in quadrature) is minimized as outlined in Ref. [32]. The correlation coefficient of 0.56 is used to multiply the statistical errors in the off-diagonal terms in the covariance matrix while the systematic errors in the same category of the two methods are conservatively taken to be fully correlated. In the combination, the decay length method lifetime measurement is weighted by a factor of 0.76 and the impact parameter method measurement by 0.24. The systematic errors in the same category of the two methods are added linearly according to the weights and then combined in quadrature as shown in Table 4.

Weight	0.76	0.24	
Source of error	Decay Length	Impact Parameter	Combined
Primary vertex estimate	0.9%	1.7%	1.1%
Background shape and normalization	2.3%	3.3%	2.5%
b-baryon decay model	1.7%	2.5%	1.9%
b-baryon polarization	2.6%	5.4%	3.3%
Ξ_b content (b-baryon mass)	1.7%	0.8%	1.5%
Decay length estimator	2.8%	—	2.1%
b-baryon momentum estimate method	0.9%	—	0.7%
b fragmentation	—	0.4%	0.1%
Physics distribution statistics	—	3.3%	0.8%
Resolution function	—	0.8%	0.2%
Lepton efficiency	—	0.6%	0.1%
Silicon det. alignment and calib.	0.1%	0.8%	0.2%
Total systematics	5.2%	8.0%	5.5%

Table 4: *Fractional systematic errors on each measurement of the b-baryon lifetime, and in combination.*

The average b-baryon lifetime from the combination of the two methods is therefore:

$$\tau = 1.16 \pm 0.11 \pm 0.06 \text{ ps}.$$

8 Product Branching Ratio

The product branching ratio is determined using:

$$f(\mathrm{b} \to \Lambda_\mathrm{b}) \cdot BR(\Lambda_\mathrm{b} \to \Lambda \ell^- \overline{\nu} \mathrm{X}) = \frac{n_{\Lambda_\mathrm{b}}}{2\ \varepsilon_{\Lambda\ell}\ N_\mathrm{had}\ \Gamma_{\mathrm{b\overline{b}}}/\Gamma_\mathrm{had}}, \tag{12}$$

where n_{Λ_b} is the background-corrected number of identified $\Lambda\ell$ combinations arising from semileptonic b-baryon decays such as $\Lambda_\mathrm{b}^0 \to \Lambda_\mathrm{c}^+ \ell^- \overline{\nu}\mathrm{X}$, $\Lambda_\mathrm{c}^+ \to \Lambda\mathrm{X}$, $\Lambda \to \mathrm{p}\pi$; $\varepsilon_{\Lambda\ell}$ is the efficiency for identifying the correct tracks in the $\Lambda\ell$ combination from the above process in the hadronic event sample; N_had is the number of hadronic events analyzed; and $\Gamma_{\mathrm{b\overline{b}}}/\Gamma_\mathrm{had}$ is the relative production rate of $\mathrm{b\overline{b}}$ events in hadronic Z^0 decays. The selection used to identify $\Lambda\ell$ combinations from b-baryon decay was described earlier in Section 3.1 with the reminder that more restrictive electron criteria than the neural net selection are applied to decrease the systematic error due to uncertainties in the electron identification efficiency.

This measurement depends on accurate measurements of the $\Lambda\ell$ selection efficiencies and backgrounds, which are first discussed in detail. After this the numbers of candidates and the calculated product branching ratio are given. The efficiency for the selection was determined using Monte Carlo simulations. The number of observed $\Lambda\ell$ combinations from b baryons was estimated by subtracting the number of wrong-sign Λ-lepton combinations from the number of right-sign combinations and then correcting for any imbalance of the various backgrounds to the right- and wrong-sign samples.

8.1 Determination of Efficiency

Since the efficiencies for the selection criteria are correlated with one another, Monte Carlo simulated events were used to estimate the overall efficiency separately for Λe and $\Lambda\mu$ combinations. The branching ratio for $\Lambda \rightarrow p\pi$ is included in the efficiency values. Corrections to the Monte Carlo estimate were determined as described in this section resulting in efficiencies of $\epsilon_{\Lambda e} = 3.9\%$ and $\epsilon_{\Lambda\mu} = 6.0\%$. Systematic errors arise from uncertainties in the simulation of the detector response in the detector simulation program and model uncertainties at the Monte Carlo generator level. The different sources of uncertainty in the efficiency are outlined and their effects on the overall efficiency are described below.

8.1.1 Lepton-specific Selection Efficiency Uncertainties

The electron selection efficiency has been studied using both data and Monte Carlo samples [16]. After applying corrections to the resolution in the detector simulation, the Monte Carlo reproduces this relative efficiency well. The relative systematic uncertainty in the electron identification efficiency for data collected between 1990 and 1992 is 2.5% [16]. Further corrections to the electron identification efficiencies obtained using Monte Carlo simulations were found using similar methods with the data collected in 1993 and 1994. Relative corrections to the efficiencies of $(1.8 \pm 2.0)\%$ for the simulation of the 1993 data and $(4.4 \pm 2.0)\%$ for the simulation of the 1994 data were applied, leading to an overall systematic uncertainty of $\Delta\varepsilon_{\Lambda e}/\varepsilon_{\Lambda e} = 3.0\%$.

The determination of the efficiency for the muon identification is discussed in detail in Refs. [16, 20]. The efficiency obtained from Monte Carlo simulations is estimated to have a relative uncertainty of 1.7%. In addition, tracking errors affecting the muon impact parameter requirement and the matching efficiency were found to be described in the Monte Carlo simulation within a systematic uncertainty of 1.6% leading to an overall systematic uncertainty of $\Delta\varepsilon_{\Lambda\mu}/\varepsilon_{\Lambda\mu} = 2.3\%$.

The rates for selected electron and muon candidates were compared between different years of data taking and were shown to have systematic fluctuations of less than 1%, which are well contained in the assigned systematic errors. Table 5 summarizes the systematic errors on the efficiencies for detecting Λe or $\Lambda\mu$ combinations, including the uncertainty contribution arising from the limited Monte Carlo sample sizes.

8.1.2 Uncertainty in Λ Selection Efficiency

Most of the selection criteria used in the Λ identification algorithm are based on tracking quantities measured in the r-ϕ plane of the central detector. The sensitivity of the Λ selection efficiency to uncertainties in the azimuthal angle and impact parameter tracking resolutions was tested by varying the smearing factors described in Section 3.2 between 1.0 and 1.6 for f_{ϕ_0} between 1.0 and 1.8 for f_{d_0}. The observed change in selection efficiency of $\Delta\varepsilon_{\Lambda\ell}/\varepsilon_{\Lambda\ell} = 3.0\%$ was independent of Λ momentum, and was taken as a systematic error due to tracking uncertainties.

Source	Systematic Error, $\Delta\varepsilon_{\Lambda\ell}/\varepsilon_{\Lambda\ell}$	
	Λe	$\Lambda\mu$
Monte Carlo Statistics	2.0%	1.6%
Lepton Identification	3.0%	2.3%
Total	3.6%	2.8%

Table 5: *Uncorrelated systematic errors on the efficiencies used for the product branching ratio analysis. All numbers are relative to the efficiency obtained from the Monte Carlo simulation.*

Systematic effects due to the additional criteria of requiring good z-information for the tracks, of demanding consistency of the measured $\mathrm{d}E/\mathrm{d}x$ of the proton candidate with the proton hypothesis, the K^0_S rejection cut, and the Λ invariant mass cut were estimated by comparing data and Monte Carlo in different momentum intervals. An empirical function that models the signal as well as the background shape was fitted to the pπ invariant mass distribution separately in both the data and the Monte Carlo events. The number of signal candidates satisfying the selection requirements and the number of candidates rejected by the requirements were found. Relative efficiencies determined in this way separately in both the data and Monte Carlo samples were then compared.

The observed mass resolution is wider in the data than in the Monte Carlo samples, mostly due to the better p_z resolution in the Monte Carlo. Following the mass window cut, the efficiency was found to be $(5.5 \pm 0.6)\%$ lower in the data than in the Monte Carlo for the region $p_\Lambda > 4$ GeV/c used in this analysis. A correction of $\delta\varepsilon_{\Lambda\ell}/\varepsilon_{\Lambda\ell} = (-5.5 \pm 0.6)\%$ is therefore applied to the overall efficiency.

8.1.3 Overall Selection Efficiencies and Other Systematic Uncertainties

The combined Λ-lepton cuts and the momentum cuts are based on kinematic quantities which are well simulated by the Monte Carlo. The efficiency of the entire selection was studied using both the unpolarized and the maximally-polarized Monte Carlo samples separately. Polarization was found to have only a minor effect on the efficiency. The efficiency obtained with -47% polarization is used for the central value of the efficiency and the maximal deviation of $\Delta\varepsilon_{\Lambda\ell}/\varepsilon_{\Lambda\ell} = 0.9\%$ between the corresponding 0% and -94% polarized samples is assigned as the systematic uncertainty due to unknown b-baryon polarization.

As described in Section 6.3, the effect of the Λ_b decay modelling was studied by using Monte Carlo samples to simulate different form factors. Differences in efficiencies between the central value using the form factor of Ref. [2] and those obtained by using an alternative theoretical form factor [27], or no form factor at all, were used to estimate a systematic error due to this source. The maximum observed difference in efficiency of 4.5% is assigned as the systematic uncertainty.

The effect of uncertainties in b-quark fragmentation for the determination of the total efficiency was studied by reweighting the Monte Carlo samples using different ϵ_b parameters of the Peterson fragmentation function [24] from that which was used for their generation. The selection efficiency obtained with the value of $\epsilon_\mathrm{b} = 0.0055$ was used for the central value and the maximal difference in efficiency of 3.0% obtained with values of $\epsilon_\mathrm{b} = 0.0025$ and $\epsilon_\mathrm{b} = 0.0095$ [19] is assigned as the systematic error due to the uncertainty in fragmentation.

In the generation of the Monte Carlo samples the value $m_{\Lambda^0_\mathrm{b}} = 5620$ MeV/c^2 was used. To study the effects on the selection efficiency of different choices of the b-baryon masses as discussed in Section 6.5, Monte Carlo studies were performed by varying the default mass of each b baryon by

± 100 MeV/c^2, resulting in an observed change in efficiency of up to 1.8%, which is included as a systematic error.

Simulated semileptonic Λ_b decays were always of the form $\Lambda_b^0 \to \Lambda_c^+ \ell^- \overline{\nu} X$. In principle, one would also expect to find decays of the form $\Lambda_b^0 \to Y_c \ell^- \overline{\nu} X$ in which Y_c is an excited c baryon state, or decays involving additional pions. However, decays including additional pions should occur with only small probability. Most likely are decays into Σ_c^+ or Σ_c^{*+}. From simple spin arguments one expects a ratio of $\Sigma_c^+ : \Sigma_c^{*+} = 1:2$. The decays $\Lambda_b \to \Lambda_c^+$ and $\Lambda_b \to \Sigma_c^+$ are assumed to occur equally often, because of the nearly equal rates of the analog $\Lambda_c^+ \to \Lambda\pi^+$ and $\Lambda_c^+ \to \Sigma^0\pi^+$ decays. A Σ_c^{*+} decays electromagnetically into $\Sigma_c^+\gamma$ followed by $\Sigma_c^+ \to \Lambda_c^+\pi^0$. Monte Carlo simulations were used to estimate the effect on the selection efficiency. In specially-generated Monte Carlo samples, such Λ_b^0 decays were simulated using the EURODEC program with appropriately modified decay tables. A decrease in efficiency of $(2.6 \pm 0.8)\%$, where the error is due to Monte Carlo statistics, was found using the above ratios. The selection efficiency has been corrected by $\delta\varepsilon_{\Lambda\ell}/\varepsilon_{\Lambda\ell} = (-1.3 \pm 1.3)\%$ to encompass the full range of possible decay rates.

In the Monte Carlo samples, it was found that 12% of all semileptonic b-baryon decays are Ξ_b decays. The selection efficiency for Λ-lepton pairs from Ξ_b baryons is expected to be smaller than for those from Λ_b^0 decay chains since roughly 50% of the Ξ_b baryons will decay via the chain $\Xi_b \to \Xi_c \to \Xi \to \Lambda$. The Ξ baryons have lifetimes comparable to that of the Λ itself and will therefore decay into a Λ at large radii in the detector, leading to an overall smaller selection efficiency for the Λ. The effect on the efficiency was studied by allowing the Ξ_b rate in the Monte Carlo to vary between 0% and 24%. Changes of $\Delta\varepsilon_{\Lambda\ell}/\varepsilon_{\Lambda\ell} = 2.4\%$ were found in comparison to the value obtained with the default 12% Ξ_b content. This variation is assigned as the systematic error due to the unknown Ξ_b content. A Ξ_b content of 12% is used for the central value of the efficiency.

The branching ratios of the decay modes $\Lambda_c^+ \to \Lambda X$ are not well known. Different decay chains could lead to different momentum distributions of the resulting Λ and therefore to different selection efficiencies. In order to check the effects of different decay modellings, Λ_c^+ decays simulated with EURODEC using the updated decay tables described in Section 3.2 were compared to those simulated with JETSET default decay tables. The resulting observed difference in efficiency of $\Delta\varepsilon_{\Lambda\ell}/\varepsilon_{\Lambda\ell} = (+1.1 \pm 1.9)\%$, where the error is due to Monte Carlo statistics, is small and is conservatively assigned as the systematic error due to uncertainties in the Λ_c^+ decay modelling.

In summary the efficiencies obtained for the Λ-electron and Λ-muon samples are:

$$\varepsilon_{\Lambda e} = 0.0378 \pm 0.0014 \pm 0.0028; \quad \varepsilon_{\Lambda\mu} = 0.0602 \pm 0.0017 \pm 0.0044,$$

where the first error represents the combined uncertainty due to limited Monte Carlo statistics and the lepton identification specific uncertainty shown in Table 5, and the second error represents all the other systematic uncertainties in the efficiency determination as summarized in Table 6. The first errors are assumed to be uncorrelated to each other while the second errors are fully correlated.

8.2 Background

There are several background sources that have a signature similar to that of the signal. Some of these backgrounds contribute equally to the right-sign and wrong-sign sample and are therefore easily accounted for by subtracting the number of events in the wrong-sign sample from the number in the right-sign sample. Other backgrounds contribute differently to the right-sign and the wrong-sign samples. For these, a correction to the background subtraction method was found and applied in the calculation of the product branching ratio. These are expressed in terms of the right- versus wrong-sign imbalance, $(n_r - n_w)/n_{\Lambda_b}$, where n_r and n_w are the numbers of events due to each background in the right-sign and wrong-sign samples, respectively. The following background sources were considered and are summarized in Table 7.

Source	Systematic Shift	Systematic Error $\Delta\varepsilon_{\Lambda\ell}/\varepsilon_{\Lambda\ell}$
Λ Selection:		
$BR(\Lambda \to \mathrm{p}\pi)$	–	0.1%
Track Modelling, r-ϕ-Plane	–	3.0%
Λ Mass Resolution	−5.5%	0.6%
Combined Selection:		
Λ_b Polarization	–	0.9%
Λ_b Decay Form Factor	–	4.5%
b Fragmentation	–	3.0%
Λ_b Mass	–	1.8%
Λ_b Decay Modelling	−1.3%	1.3%
Ξ_b Content	–	2.4%
Λ_c^+ Decay Modelling	–	1.9%
Total	−6.8%	7.4%

Table 6: *Corrections to the Monte Carlo prediction and systematic errors on efficiency used for the product branching ratio analysis. All numbers are relative to the efficiency obtained from the Monte Carlo simulation.*

8.2.1 Fragmentation Λ Background

Fragmentation Λ baryons combined with leptons from semileptonic c- or b-hadron decays are found to be one of the largest sources of background. In the framework of string fragmentation and the "popcorn" model [33], as implemented in the JETSET Monte Carlo program, it is expected that these backgrounds contribute differently to the right-sign and wrong-sign samples. Take as an example a b-baryon semileptonic decay $\Lambda_\mathrm{b} \to \Lambda_\mathrm{c}^+ \ell^- \overline{\nu} \mathrm{X}$ followed by $\Lambda_\mathrm{c}^+ \to \Lambda \mathrm{X}$. In a string-like model, an anti-baryon is necessarily formed in the fragmentation process and will tend to have fairly high momentum since it will be among the first few particles formed in the fragmentation chain. If it is a $\overline{\Lambda}$ and passes the kinematic cuts, then the fragmentation $\overline{\Lambda}\ell^-$ combination will enter the wrong-sign sample and not the right-sign sample. If a c-meson decays semileptonically into a ℓ^+ and a Λ-$\overline{\Lambda}$ baryon pair is formed during fragmentation, the Λ will tend to have a higher momentum than the $\overline{\Lambda}$ and have a higher selection probability resulting in a preferential population of the wrong-sign sample with this background. Similar arguments hold true for fragmentation Λ baryons combined with leptons from B-meson or c-baryon decay that tend to contribute more to the right-sign sample. The imbalances predicted by Monte Carlo studies are shown in Table 7.

To study modelling effects, these background source Monte Carlo studies were repeated using the JETSET input parameters given in [34], corresponding to 0% popcorn and a 95% popcorn model parameter [33]. The popcorn parameter is the probability that mesons are produced between baryon pairs and therefore determines the degree of correlation between the baryon pairs and the momentum spectrum of fragmentation Λ baryons. To keep the baryon production rates in agreement with the data, the parameters controlling strange diquark production and the spin-1 versus spin-0 production were also adjusted accordingly [34]. The result of these popcorn model parameter variations is included in the total error for the fragmentation Λ background imbalance in Table 7. An imbalance of $(n_r - n_w)/n_{\Lambda_\mathrm{b}} = (-11.8 \pm 1.3 \pm 2.6)\%$ is predicted, due to this specific background. The first error accounts for limited Monte Carlo statistics and the second error is the systematic uncertainty reflecting the difference seen between the default 50% and 95% probability values for popcorn.

As a check of the accuracy of the Monte Carlo estimate, the data sample was searched for pairs of candidates that had the same lepton but different Λ candidates. Five such events were found, and as expected, they all had one Λ and one $\overline{\Lambda}$ candidate. Monte Carlo simulation predicts 6.4 ± 0.7 such events.

Imbalance, $\delta = (n_r - n_w)/n_{\Lambda_b}$		
Background	Imbalance	Correction
Fragmentation Λ plus:		
ℓ from B meson	$+(2.5\pm1.0)\%$	
ℓ from c baryon	$+(1.2\pm0.2)\%$	
ℓ from b baryon	$-(11.9\pm0.6)\%$	
ℓ from c meson	$-(3.4\pm0.6)\%$	
Subtotal:		$-(11.8\pm1.3\pm2.6)\%$
Exclusive Backgrounds:		
$\Lambda_b \to \Lambda_c^+ \tau^- \overline{\nu}$	$+(1.8\pm0.2)\%$	
	$+(1.2\pm0.6)\%$	
$\overline{B} \to Y_c \overline{N} \ell^- X$	$+(1.4\pm1.4)\%$	
$\overline{B} \to \Lambda \overline{p} X$	Negligible	
$\Lambda_c^+ \to \Lambda \ell^+ \nu$	$-(2.5\pm0.3)\%$	
Subtotal :		$+(1.9\pm1.6)\%$
Combinatorials and Fakes:		$+(1.1\pm0.5)\%$
Total δ:		$-(8.8\pm3.3)\%$

Table 7: *Corrections to the wrong-sign subtraction method obtained for different classes of backgrounds. The error on the correction for the fragmentation Λ plus lepton includes varying the 'popcorn' parameter as described in the text. The percentages are each with respect to the number of real identified $\Lambda\ell$ combinations from b baryons in each class and are additive.*

8.2.2 Exclusive Decay Channel Background

In addition to the fragmentation Λ background, several exclusive decay channels which contribute unequally to the right-sign and wrong-sign samples must be considered. The contributions from these exclusive decay channels, which are described below and listed in Table 7, are small compared to the previously described fragmentation backgrounds.

Semileptonic decay of a b baryon into a τ which then decays leptonically is not counted as a signal combination, but still populates only the right-sign sample. Differences in phase space for $b \to \tau$ decays and the leptonic τ branching ratios are well-known and the indicated imbalance is estimated using Monte Carlo events. The same sample is used to find the contribution from $\Lambda_b \to \Lambda_c^+ D_s^-$ followed by $D_s^- \to \ell^- X$. Since little is known about the branching ratio for $\Lambda_b \to \Lambda_c^+ D_s^-$, a systematic uncertainty of 50% is taken for the branching ratio used in the simulation.

The process $\overline{B} \to Y_c \overline{N} \ell^- \overline{\nu}$, where Y_c is a c baryon and $\overline{N}$ is an anti-baryon, is a potential background that has not been observed. An upper limit of $BR(B \to \overline{p} e^+ \nu X) < 0.16\%$ (90% *C.L.*) has been measured by the ARGUS collaboration [35]. Using the ansatz:

$$BR(\overline{B} \to \Lambda \ell^- X)/BR(\overline{B} \to p \ell^- X) = BR(\overline{B} \to \Lambda X)/BR(\overline{B} \to pX), \tag{13}$$

and the measurements $BR(\overline{B} \to \Lambda X) = (4.0 \pm 0.5)\%$, and $BR(\overline{B} \to pX) = (8.0 \pm 0.5)\%$ [22] as input parameters for a Monte Carlo simulation, an upper limit on the contribution of this background to

the right-sign sample is found to be 2.8%, and a correction of $(1.4 \pm 1.4)\%$ is applied to encompass the entire possible range.

A potential background can result from $\overline{\mathrm{B}} \to \Lambda\overline{\mathrm{p}}\mathrm{X}$ where the $\overline{\mathrm{p}}$ is subsequently misidentified as a lepton. By studying the $\mathrm{d}E/\mathrm{d}x$ distributions in the general Monte Carlo sample, this misidentification probability was determined to be small. From Monte Carlo studies using the measurement of $BR(\overline{\mathrm{B}} \to \Lambda\overline{\mathrm{p}}\mathrm{X}) = (2.5 \pm 0.4)\%$ [22], the contribution to the $\Lambda\mu$ signal is predicted to be of the order of 0.2 events, and for the Λe signal it is even smaller. This background is therefore negligible.

The contribution to the wrong-sign sample by semileptonically decaying c baryons is kept small by the $\Lambda\ell$ invariant mass criterion. The systematic error on this imbalance is small since most b baryons decay via c baryons into Λ baryons, and decay modelling effects cancel out in the calculation of the ratio.

A combined imbalance of $(+1.9 \pm 1.6)\%$ is predicted for the exclusive decay channels considered.

8.2.3 Combinatorial Background and Backgrounds from Fakes

Another background is due to random combinations of tracks. Fakes due to leptons or Λ baryons that have been misidentified are also present. The total contribution of these backgrounds is of similar size to the contribution from the fragmentation Λ baryons, but in contrast these backgrounds are assumed to contribute equally to the right-sign and wrong-sign samples. This hypothesis has been tested with the fully-simulated hadronic Monte Carlo sample and is found to be correct within the statistical uncertainty. Cross-checks in the data side-bands of the $\mathrm{p}\pi$ invariant mass distribution also verify the hypothesis.

A potential background arises if the lepton from the semileptonic $\Lambda_\mathrm{b} \to \Lambda\ell\mathrm{X}$ decay and one of the tracks from the $\Lambda \to \mathrm{p}\pi$ decay have been correctly identified, but the second track (usually the π) is misidentified. Since the presence of a Λ or $\overline{\Lambda}$ is distinguished by the charge of the proton candidate, such events would preferentially populate the right-sign sample. In the determination of the efficiency, only combinations where all three of the proton, pion, and lepton tracks are correctly identified are considered as signal. The magnitude of the effect was studied by searching for 'double' $\Lambda\ell$ combinations associated with the same jet in the data sample where two $\Lambda\ell$ combinations include the same lepton and either the same proton but different pion tracks, or the same pion but different proton tracks. Monte Carlo studies show that in 63% of cases where a $\Lambda\ell$ combination with a fake pion track is selected, a candidate including the correct pion is selected too, resulting in two combinations. From the occurrences of such double combinations in the data, a contribution to the right-sign sample of 5 ± 2 events from this background is estimated, leading to a predicted imbalance of $(+1.1 \pm 0.5)\%$.

Contributions from hadronic decays of b baryons where leptons are produced via decays of secondary particles into leptons pairs (from, e.g., $\mathrm{J}/\psi \to \ell^+\ell^-$) are small, but it has been checked that these backgrounds contribute to the right-sign and wrong-sign samples equally.

8.2.4 Total Background Correction

A summary of all classes of backgrounds is shown in Table 7. The total correction to the wrong-sign subtraction method of $\delta = (n_r - n_w)/n_{\Lambda_\mathrm{b}} = (-8.8 \pm 3.3)\%$ is found. In this total correction, n_w is the total number of events in the wrong-sign sample, and n_r is the total number of background events in the right-sign sample.

8.3 Product Branching Ratio Result

In the data sample collected by OPAL in the years 1990 to 1994, 268 right-sign Λe^- and 466 right-sign $\Lambda\mu^-$ combinations were found, while in the wrong-sign sample 128 Λe^+ and 199 $\Lambda\mu^+$ combinations were identified. The number of observed $\Lambda\ell$ combinations, n_{Λ_b}, from b-baryon semileptonic decays is calculated, taking into account the expected imbalance between the backgrounds in the right- and wrong-sign samples, $\delta = (-8.8 \pm 3.3)\%$, by using $n_{\Lambda_b} = (N_r - N_w)/(1+\delta)$, where N_r and N_w are the numbers of observed events in the right-sign and wrong-sign sample, respectively. The resulting numbers of signal events are:

$$n^{e}_{\Lambda_b} = 154 \pm 22 \pm 5; \quad n^{\mu}_{\Lambda_b} = 293 \pm 28 \pm 10,$$

where the first errors are statistical and the second errors are due to the background correction.

Using Eq. 12 and the OPAL measurement of $\Gamma_{b\bar{b}}/\Gamma_{had} = 0.2171 \pm 0.0030$ [16], the following results are obtained:

$$f(b \to \Lambda_b) \cdot BR(\Lambda_b \to \Lambda e^- \overline{\nu} X) = (2.59 \pm 0.37 \pm 0.23) \cdot 10^{-3},$$
$$f(b \to \Lambda_b) \cdot BR(\Lambda_b \to \Lambda \mu^- \overline{\nu} X) = (3.10 \pm 0.30 \pm 0.27) \cdot 10^{-3},$$

where the first errors are due to limited statistics and the second to systematic uncertainties. The systematic uncertainties are dominated by the uncertainties in the determination of the selection efficiencies.

The results for electrons and muons are expected to be equal. Taking all correlations into account, the χ^2 of the two measurements is found to be 1.1. Combining the results, taking into account their common systematic errors, the result

$$f(b \to \Lambda_b) \cdot BR(\Lambda_b \to \Lambda \ell^- \overline{\nu} X) = (2.91 \pm 0.23 \pm 0.25) \cdot 10^{-3}$$

is obtained, where the symbol ℓ represents either an electron or muon, and where the first error is statistical and the second systematic.

As a cross check, the electron analysis was repeated using the more efficient neural net electron selection (see Section 3.1). The result is consistent with that given above, but despite the smaller statistical error, the total error is larger due to the larger systematic uncertainties for the neural net selection efficiency.

This combined result supersedes the previously published OPAL result [9] of $(2.9 \pm 0.5 \pm 0.7) \cdot 10^{-3}$ which was based on only the 1990–1991 data. Repeating the present analysis on this earlier data set gives a result of $(3.4 \pm 0.6 \pm 0.3) \cdot 10^{-3}$. The largest differences with respect to the previous method are due to inclusion of the correction for the imbalance in the background estimate $(+9.6\%)$ and the use of a form factor to model the energy transfer from the Λ_b to the Λ_c in the determination of the overall efficiency $(+5\%)$.

9 Discussion and Conclusions

The OPAL measurement of the average b-baryon lifetime is updated using two different methods. A sample of Λ-lepton combinations with correlations between Λ baryon number and lepton charge, indicating the presence of a semileptonic b-baryon decay, is first isolated. The observed decay length distribution between the primary vertex and the Λ-lepton vertex and the impact parameter distribution of the leptons are used to determine the average b-baryon lifetime:

$$\tau = 1.16 \pm 0.11 \pm 0.06 \text{ ps},$$

where the first error is statistical and the second systematic.

This result represents a substantial improvement over the previously published OPAL result of $\tau = 1.05^{+0.23}_{-0.20} \pm 0.08$ ps [10]. Figure 6 compares this result to other OPAL measurements [7] of lifetimes of exclusive B mesons, to an OPAL lifetime measurement obtained from a sample of Λ_c-lepton combinations that provides a purer sample of Λ_b^0 decays [6], and to the OPAL inclusive b hadron lifetime measurement [4]. The presented result is consistent with results from other experiments [8] and is also more precise. When OPAL's Λ_b^0 lifetime measurement [6] is combined with the presented result, an average lifetime of 1.16 ± 0.11 ps is found, where the error is the combined statistical and systematic uncertainty. A trend towards shorter lifetimes of b baryons compared with lifetimes of other B mesons is evident.

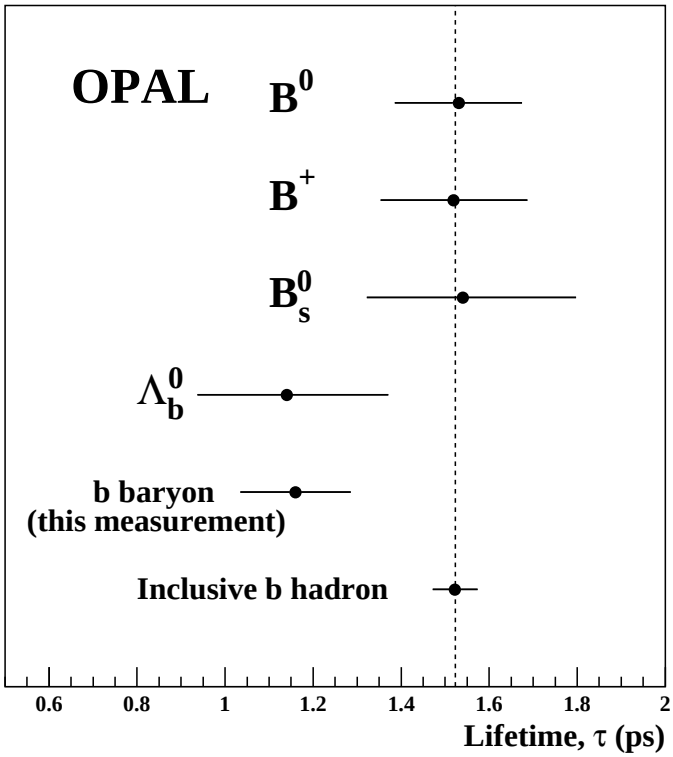

Figure 6: *The average b-baryon lifetime presented here compared to other OPAL b hadron lifetime measurements.*

A similar sample of Λ-lepton combinations is used to determine the product branching ratio

$$f(\mathrm{b} \to \Lambda_\mathrm{b}) \cdot BR(\Lambda_\mathrm{b} \to \Lambda \ell^- \overline{\nu} \mathrm{X}) = (2.91 \pm 0.23 \pm 0.25) \cdot 10^{-3},$$

where the symbol ℓ represents either an electron or a muon and $f(\mathrm{b} \to \Lambda_\mathrm{b})$ is the fraction of b quarks from Z^0 decays forming b baryons. This result supersedes the previously published OPAL result [9], and is consistent with results from other experiments [8]. Using the measured branching ratio $BR(\Lambda_c^+ \to \Lambda \mathrm{X}) = (35 \pm 11)\%$ [22], one obtains: $f(\mathrm{b} \to \Lambda_\mathrm{b}) \cdot BR(\Lambda_\mathrm{b} \to \Lambda_c^+ \ell^- \overline{\nu} \mathrm{X}) = (8.3 \pm 2.8) \cdot 10^{-3}$, under the assumption that all semileptonically decaying b baryons decay into c baryons as an intermediate state, and that the c baryons have the same branching ratios into Λ as the Λ_c^+. Typical theoretical estimates of $BR(\Lambda_\mathrm{b} \to \Lambda_c^+ \ell^- \overline{\nu} \mathrm{X})$ range from 2.45% [2] to 10–13% [27] indicating the strong need for a measurement of this branching ratio to allow the reliable extraction of $f(\mathrm{b} \to \Lambda_\mathrm{b})$ from the measured product branching ratio. Further measurements of such quantities as $BR(\mathrm{b\ hadron} \to \Lambda \mathrm{X})$ and $BR(\Lambda_\mathrm{b} \to \Lambda \ell^- \overline{\nu} \mathrm{X})$ are important to place constraints on $f(\mathrm{b} \to \Lambda_\mathrm{b})$ and $BR(\Lambda_\mathrm{b} \to \Lambda_c^+ \ell^- \overline{\nu} \mathrm{X})$.

10 Acknowledgements

It is a pleasure to thank the SL Division for the efficient operation of the LEP accelerator and their continuing close cooperation with our experimental group. In addition to the support staff at our own institutions we are pleased to acknowledge the

Department of Energy, USA,
National Science Foundation, USA,
Particle Physics and Astronomy Research Council, UK,
Natural Sciences and Engineering Research Council, Canada,
Fussefeld Foundation,
Israel Ministry of Science,
Israel Science Foundation, administered by the Israel Academy of Science and Humanities,
Minerva Gesellschaft,
Japanese Ministry of Education, Science and Culture (the Monbusho) and a grant under the Monbusho International Science Research Program,
German Israeli Bi-national Science Foundation (GIF),
Direction des Sciences de la Matière du Commissariat à l'Energie Atomique, France,
Bundesministerium für Forschung und Technologie, Germany,
National Research Council of Canada,
A.P. Sloan Foundation and Junta Nacional de Investigação Científica e Tecnológica, Portugal.

References

[1] R. Rückl, in *Z Physics at LEP 1*, Vol. 1, CERN 89-08 (1989) p. 311;
I. Bigi and N.G. Uraltsev, Phys. Lett. **B280** (1992) 271;
I. Bigi *et al.*, *Non-Leptonic Decays of Beauty Hadrons – From Phenomenology to Theory*, (CERN-TH.7132/94), from the second edition of the book 'B Decays', S. Stone (ed.), World Scientific, pp. 132-157.

[2] X.H. Guo and P. Kroll, Z. Phys. **C59** (1993) 567.

[3] ALEPH Collab., D. Buskulic *et al.*, Phys. Lett. **B314** (1993) 459;
ALEPH Collab., D. Buskulic *et al.*, Phys. Lett. **B295** (1992) 174;
CDF Collab., F. Abe *et al.*, Phys. Rev. Lett. **71** (1993) 3421;
DELPHI Collab., P. Abreu *et al.*, Z. Phys. **C63** (1993) 3;
L3 Collab., O. Adriani *et al.*, Phys. Lett. **B317** (1993) 474.

[4] OPAL Collab., P.D. Acton *et al.*, Z. Phys. **C60** (1993) 217.

[5] ALEPH Collab., D. Buskulic, *et al.*, Phys. Lett. **B307** (1993) 194;
ALEPH Collab., D. Buskulic, *et al.*, Phys. Lett. **B322** (1994) 275;
CDF Collab., F. Abe *et al.*, Phys. Rev. Lett. **72** (1994) 3456;
CDF Collab., F. Abe *et al.*, *Measurement of the* B_s *Meson Lifetime*, FERMILAB-PUB-94/420-E, January 1995 submitted to Phys. Rev. Lett.;
DELPHI Collab., P. Abreu *et al.*, Z. Phys. **C61** (1994) 407;
DELPHI Collab., P. Abreu *et al.*, *Lifetimes of Charged and Neutral B Hadrons Using Event Topology*, CERN-PPE/95-59 (28 Apr. 1995), submitted to Z. Phys. C;
DELPHI Collab., P. Abreu *et al.*, *A Measurement of* B^+ *and* B^0 *Lifetimes using* $\overline{D}\ell^+$ *events*, CERN-PPE/95-60 (3 May 1995), submitted to Z. Phys. C.

[6] OPAL Collab., R. Akers *et al.*, *A Measurement of the* Λ_b^0 *Lifetime*, CERN-PPE/95-051 (13 Apr. 95), accepted by Phys. Lett. B.

[7] OPAL Collab., R. Akers *et al.*, *Improved Measurements of the* B^0 *and* B^+ *Lifetimes*, CERN-PPE/95-019 (22 Feb. 1995), accepted by Z. Phys. C;
OPAL Collab., R. Akers *et al.*, Phys. Lett. **B350** (1995) 273.

[8] ALEPH Collab., D. Buskulic *et al.*, *Measurements of the b Baryon Lifetime*, CERN-PPE/95-65 (2 May 1995), submitted to Phys. Lett. B;
DELPHI Collab., P. Abreu *et al.*, *Lifetime and production rate of beauty baryons from Z decays*, CERN-PPE/95-54 (21 Apr. 1995), submitted to Z. Phys. C.

[9] OPAL Collab., P.D. Acton *et al.*, Phys. Lett. **B281** (1992) 394.

[10] OPAL Collab., R. Akers *et al.*, Phys. Lett. **B316** (1993) 435.

[11] OPAL Collab., K. Ahmet *et al.*, Nucl. Inst. and Meth. **A305** (1991) 275;
O. Biebel *et al.*, Nucl. Inst. and Meth. **A323** (1992) 169.

[12] M. Hauschild *et al.*, Nucl. Inst. and Meth. **A314** (1992) 74.

[13] P.P. Allport *et al.*, Nucl. Inst. and Meth. **A324** (1993) 34.

[14] P.P. Allport *et al.*, Nucl. Inst. and Meth. **A346** (1994) 476.

[15] OPAL Collab., G. Alexander *et al.*, Z. Phys. **C52** (1991) 175.

[16] OPAL Collab., R. Akers *et al.*, Z. Phys. **C65** (1995) 17.

[17] OPAL Collab., M.Z. Akrawy *et al.*, Phys. Lett. **B263** (1991) 311.

[18] OPAL Collab., R. Akers *et al.*, Phys. Lett. **B327** (1994) 411.

[19] OPAL Collab., R. Akers *et al.*, Z. Phys. **C60** (1993) 199.

[20] OPAL Collab., P.D. Acton *et al.*, Z. Phys. **C58** (1993) 523.

[21] JADE Collab., W. Bartel *et al.*, Z. Phys. **C33** (1986) 23;
JADE Collab., S. Bethke *et al.*, Phys. Lett. **B213** (1988) 235;
OPAL Collab., M.Z. Akrawy *et al.*, Z. Phys. **C49** (1991) 375.

[22] Particle Data Group, *Review of Particle Properties*, Phys. Rev. **D50** (1994) 1173.

[23] T. Sjöstrand, *The JETSET 7.3 Manual*, CERN-TH.6488/92;
T. Sjöstrand, Comp. Phys. Comm. **39** (1987) 347;
T. Sjöstrand and M. Bengtsson, Comp. Phys. Comm. **43** (1987) 367;
OPAL optimized parameters were used, as described in
OPAL Collab., M.Z. Akrawy *et al.*, Z. Phys. **C47** (1990) 505.

[24] C. Peterson, D. Schlatter, I. Schmitt and P.M. Zerwas, Phys. Rev. **D27** (1983) 105.

[25] A. Ali and B. van Eijk in *Z Physics at LEP 1*, Vol. 3, CERN 89-08 (1989) p. 226.

[26] Particle Data Group, *Review of Particle Properties*, Phys. Rev. **D45** (1992) 1.

[27] T. Mannel and G. Schuler, Phys. Lett. **B279** (1992) 194;
T. Sjöstrand, private communication;
S. Jadach and Z. Was, in *Z Physics at LEP 1*, Vol. 1, CERN 89-08 (1989) p. 235.

[28] J. Allison *et al.*, Nucl. Inst. Meth. **A317** (1992) 47.

[29] OPAL Collab., P.D. Acton *et al.*, Z. Phys. **C59** (1993) 183.

[30] DELPHI Collab., P. Abreu *et al.*, *Production of strange B-baryons decaying into* $\Xi^{\mp} - \ell^{\mp}$ *pairs at LEP*, CERN-PPE/95-29 (16 Mar. 1995), submitted to Z. Phys. C.

[31] W. Kwong and J. Rosner, Phys. Rev. **D44** (1991) 212, and references therein.

[32] L. Lyons, D. Gibaut, and P. Clifford, Nucl. Inst. Meth. **A270** (1988) 110.

[33] B. Andersson, G. Gustafson and T. Sjöstrand, Physica Scripta **32** (1985) 574.
A popcorn model has been implemented in JETSET, where the frequency for the process baryon-meson-antibaryon is regulated in JETSET by the parameter PARJ(5), such that the probability is given by PARJ(5)/(0.5 + PARJ(5)).

[34] OPAL Collab., P.D. Acton *et al.*, Phys. Lett. **B 305** (1993) 415.

[35] ARGUS Collab., H. Albrecht *et al.*, Phys. Lett. **B 249** (1990) 359.